© 2015. Published by The Company of Biologists Ltd | Development (2015) 142, 597-606 doi:10.1242/dev.114603

RESEARCH ARTICLE

TECHNIQUES AND RESOURCES

CoinFLP: a system for efficient mosaic screening and for visualizing clonal boundaries in *Drosophila*

Justin A. Bosch, Ngoc Han Tran and Iswar K. Hariharan*

ABSTRACT

Screens in mosaic *Drosophila* tissues that use chemical mutagenesis have identified many regulators of growth and patterning. Many of the mutant phenotypes observed were contingent upon the presence of both wild-type and mutant cells in the same tissue. More recently, large collections of RNAi lines or cDNAs expressed under Gal4/*UAS* control have been used to alter gene expression uniformly in specific tissues. However, these newer approaches are not easily combined with the efficient generation of genetic mosaics. The CoinFLP system described here enables mosaic screens in the context of gene knockdown or overexpression by automatically generating a reliable ratio of mutant to wild-type tissue in a developmentally controlled manner. *CoinFLP-Gal4* generates mosaic tissues composed of clones of which only a subset expresses Gal4. *CoinFLP-LexGAD/Gal4* generates tissues composed of clones that express either Gal4 or LexGAD, thus allowing the study of interactions between different types of genetically manipulated cells. By combining *CoinFLP-LexGAD/Gal4* with the split-GFP system GRASP, boundaries between genetically distinct cell populations can be visualized at high resolution.

KEY WORDS: *Drosophila*, RNAi, Boundary, Mosaic screen, Overexpression

INTRODUCTION

Many of the genes that regulate development in a variety of organisms have been discovered in genetic screens that utilize the *Drosophila* eye (St Johnston, 2002). An important advance in the design of these screens was the development of methods that allow the generation of eyes bearing homozygous mutant clones (Golic, 1991; Newsome et al., 2000; Xu and Rubin, 1993). This enabled investigators to restrict the deleterious effects of the mutation to a tissue that was not essential for viability or fertility. As a result, mosaic screens in the *Drosophila* eye have discovered many genes that function in regulating cell proliferation, cell fate specification and photoreceptor differentiation (e.g. Benlali et al., 2000; Tapon et al., 2001; Treisman, 2001).

We now know that there are mutations in several types of genes that function in cell-cell interactions whose effects could only have been discovered in a tissue consisting of two different types of cells (wild type and mutant). These include important subgroups of genes that regulate cell proliferation and the affinity of cell-cell interactions. These mutant phenotypes become evident by changes in the relative representation of the two populations (Tseng et al., 2007), by overgrowth of one population induced by its interaction with the other (Lee et al., 2002), or by abnormalities in the boundaries that separate the two populations (e.g. smooth rather than irregular) (Yang et al., 1999). Importantly, these abnormalities would not have been evident if the entire eye was composed of mutant tissue.

The Gal4/*UAS* binary expression system in *Drosophila* (Brand and Perrimon, 1993; Fischer et al., 1988) has enabled researchers to generate mutant cells in a spatially and temporally restricted manner. In addition, it allows the systematic screening *in vivo* of thousands of Gal4-dependent *UAS* lines for mutant phenotypes, either by RNA-mediated interference (RNAi) or gene overexpression. Although RNAi and overexpression screens have been extremely effective for identifying genes in a number of complex biological processes in *Drosophila* (e.g. Colombani et al., 2012; Neely et al., 2010; Pospisilik et al., 2010), it is currently difficult to use this approach in the context of a mosaic screen.

Here we describe a new method, CoinFLP, that allows us to conduct mosaic screens in *Drosophila* tissues using RNAi or gene overexpression. This system exploits a stochastic recombination choice by the FLP enzyme to generate reliable ratios of mutant and wild-type cells in a developmentally controlled manner. We have validated this approach in the adult eye with a screen of genes that cannot be studied using the commonly used FLP/*FRT* stocks. Additionally, to facilitate the study of interactions between clones of different mutant genotypes, we have generated versions of CoinFLP that allow the simultaneous visualization of Gal4-expressing and LexGAD-expressing clones in the imaginal disc as well as the boundary between them.

RESULTS

Design and features of the CoinFLP system

In order to generate *Drosophila* tissues that are mosaic for expression of a gene of interest, we designed a system that enables the expression of Gal4 from patches of cells in a tissue and excludes its expression in the rest of the animal. We chose a FLP/*FRT*-based recombination approach to take advantage of the availability of a number of FLP-expressing stocks generated by different groups. The FLP recombinase binds to 11 bases of the inverted repeat sequence in the *FRT* element but only to the two outermost bases of the 8 bp spacer (Qian and Cox, 1995). The spacer, however, is involved in DNA-DNA pairing during the recombination event. Therefore, the central six nucleotides in the spacer can be mutated to alter the specificity of recombination. Thus, canonical *FRT* sites (shown as FRT) and *FRT3* sites (Fig. 1A) are each capable of undergoing a recombination event with a site of the same kind but not with the other type of site (Schlake and Bode, 1994; Senecoff and Cox, 1986). This type of mutually exclusive recombination between different recombinase target variants has been exploited in several genetic systems, such as iMos (Claveria et al., 2013), Brainbow (Cai et al., 2013; Hadjieconomou et al., 2011; Hampel et al., 2011; Livet et al.,

Department of Molecular and Cell Biology, University of California, Berkeley 361 LSA, Berkeley, CA 94720-3200, USA.

*Author for correspondence (ikh@berkeley.edu)

Received 23 June 2014; Accepted 5 December 2014

Development (2015) 142, 597-606 doi:10.1242/dev.114603

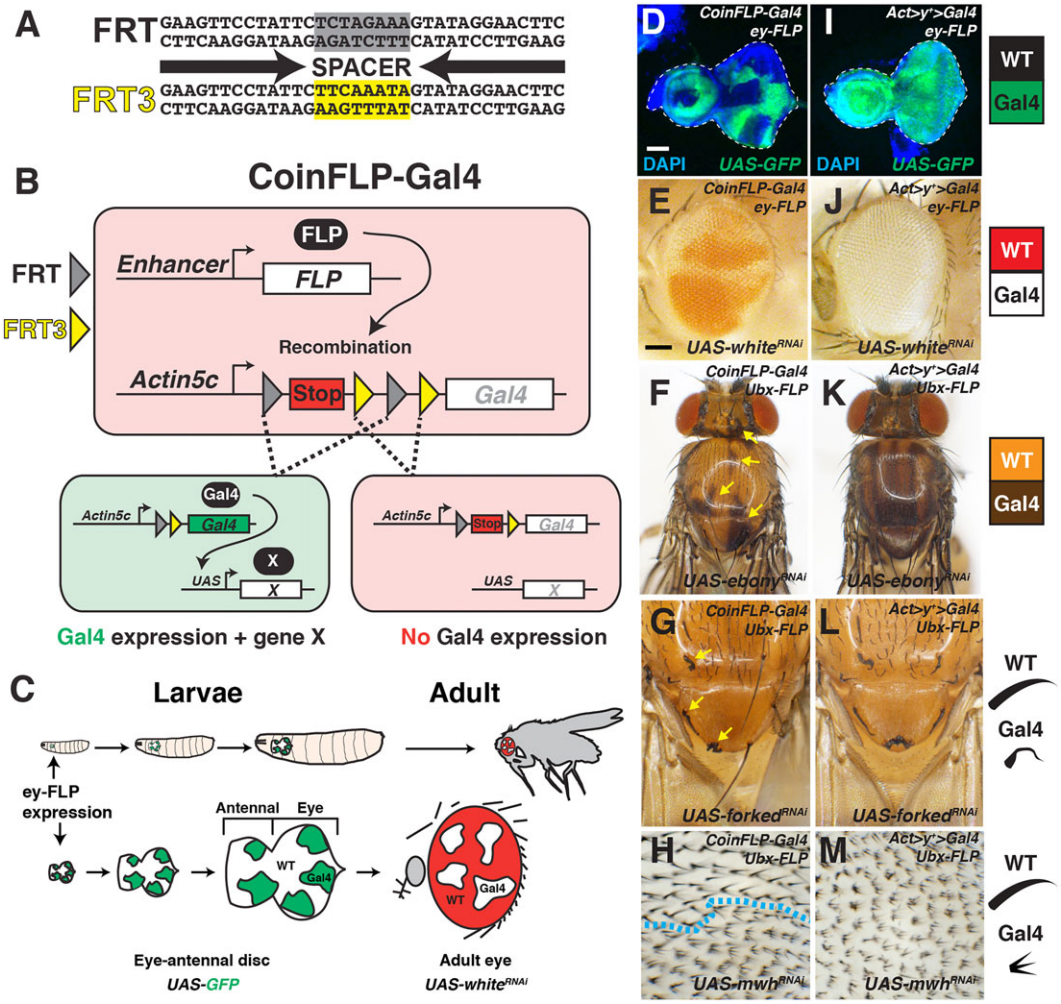

Fig. 1. The CoinFLP-Gal4 system. (A) Comparison of canonical *FRT* sites (gray) and variant *FRT3* sites (yellow). The spacer regions between the inverted repeats (highlighted) differ in sequence. (B) *CoinFLP-Gal4* used with a *FLP*-expressing transgene: recombination between canonical *FRT* sites results in excision of the STOP cassette and expression of Gal4 (green when expressed). Recombination between the *FRT3* sites excises one of the *FRT* sites and leaves the STOP cassette in place, thus preventing Gal4 expression. (C) Using *ey-FLP*, Gal4-expressing clones in the eye-antennal disc can be visualized with *UAS-GFP* (green) and in the adult eye with *UAS-white*^{RNAi} (white). Eye-antennal discs and adult eyes are positioned with anterior to the left. (D-H) Mosaics generated with *CoinFLP-Gal4* and (D,E) *ey-FLP* or (F-H) *Ubx-FLP*, with the indicated *UAS* transgenes. Arrows indicate *ebony* patches (F) or *forked* bristles (G). Blue dotted line in H indicates the boundary between wild-type bristles (above) and *mwh* bristles (below). (I-M) Uniform expression of Gal4 from recombination of *Act>y+>Gal4* with (I,J) *ey-FLP* or (K-M) *Ubx-FLP*, with the indicated *UAS* transgenes. (D,I) Eye-antennal disc with DAPI (blue), (E,J) adult eye, (F,G,K,L) adult thorax and head, and (H,M) adult wing hairs. Genotypes: (D) *ey-FLP UAS-dcr2/+; CoinFLP-Gal4 UAS-GFP/+*; (E) *ey-FLP UAS-dcr2/+; CoinFLP-Gal4/+; UAS-white*^{RNAi}*/+*; (F) *Ubx-FLP/+; CoinFLP-Gal4/+; UAS-ebony*^{RNAi}*/+*; (G) *Ubx-FLP/+; CoinFLP-Gal4/+; UAS-forked*^{RNAi}*/+*; (H) *Ubx-FLP/+; CoinFLP-Gal4/+; UAS-mwh*^{RNAi}*/+*; (I-M) Same as D-H with *Act>y+>Gal4* instead of *CoinFLP-Gal4*. Scale bars: 100 µm.

2007), recombinase-mediated cassette exchange (RMCE) (Turan et al., 2013) and the flip-excision (FlEx) transgene inversion strategy (Schnutgen et al., 2005).

We designed and constructed a system that we have named CoinFLP. The first version that we constructed was *CoinFLP-Gal4* (Fig. 1B), in which recombination between canonical *FRT* sites results in the excision of a transcriptional STOP cassette, such that the *Gal4* gene is expressed from the *Actin 5C* (*Act*) promoter in that cell and all of its descendants. By contrast, recombination between the two *FRT3* sites results in the excision of one of the canonical *FRT* sites, thus preventing any subsequent FLP/*FRT*-mediated recombination and maintaining the STOP cassette upstream of *Gal4* in that cell and all its descendants. The two types of recombination event are mutually exclusive and the choice between them is stochastic, similar to flipping a coin (hence 'CoinFLP'). The *CoinFLP-Gal4* transgene differs from the widely used FLP-out transgenes, such as *Act>CD2>Gal4* and *Act>y+>Gal4* (Ito et al., 1997; Pignoni and Zipursky, 1997; Struhl and Basler, 1993), in which recombination between *FRT* sites always results in Gal4 expression.

To generate mosaicism via *CoinFLP-Gal4*, we expressed FLP recombinase from a separate transgene. One *FLP* transgene that we used was under the control of the *eyeless* promoter (*ey-FLP*) (Newsome et al., 2000). This restricts recombination events to the developing eye-antennal imaginal disc, which gives rise to the adult eye and antenna (Fig. 1C). We empirically identified an *ey-FLP* transgene whose recombination with *CoinFLP-Gal4* was most restricted to the eye-antennal disc (Fig. 1D; supplementary material Table S1, Fig. S1A). However, we observe rare recombination events in fat body and gut cells (supplementary material Fig. S1B,C). We also tested another *FLP* transgene, *Ubx-FLP*, which is less restrictive than *ey-FLP* and induced recombination in wing, leg and eye imaginal

Development (2015) 142, 597-606 doi:10.1242/dev.114603

discs (supplementary material Fig. S1D-G). In animals bearing *ey-FLP* and *CoinFLP-Gal4*, patches of Gal4-expressing cells can be identified with different *UAS*-based markers. *UAS-GFP* fluorescently labels Gal4-expressing clones in the eye-antennal disc (Fig. 1D) and *UAS-white*^{RNAi} marks clones as white in the adult eye (Fig. 1E).

To facilitate the generation of marked patches of Gal4-expressing cells in a variety of tissues that are visible externally, we used *Ubx-FLP* and *CoinFLP-Gal4* in combination with *UAS*-regulated RNAi transgenes that affect pigmentation of the cuticle or the morphology of macrochaetae or wing hairs. *UAS-ebony*^{RNAi} marks Gal4-expressing clones with dark pigment in the adult dorsal thorax and head (Fig. 1F), *UAS-forked*^{RNAi} causes mutant patches to have bent bristles (Fig. 1G), and *UAS-mwh*^{RNAi} marks clones with multiple hairs in the wing (Fig. 1H). By comparison, the *Act>y+>Gal4* transgene causes most, if not all, cells expressing FLP to express Gal4 in a non-mosaic uniform pattern (Fig. 1I-M). These results demonstrate that *CoinFLP-Gal4* is a versatile tool that can be used to generate and visualize Gal4-expressing clones in a variety of tissues when paired with the desired *UAS*-regulated marker and tissue-specific FLP.

One of the benefits of traditional mitotic recombination using *ey-FLP* (Newsome et al., 2000) is that a predictable proportion of mutant cells is generated, which has allowed the identification of mutations that cause a significant deviation from the expected ratio (Tapon et al., 2001). When compared with clones generated by mitotic recombination using *ey-FLP* (supplementary material Fig. S1H,I), clones generated using *CoinFLP-Gal4* are fewer and larger (Fig. 1D and see below). This might be because recombination between *FRT* sites in *cis* occurs at an earlier stage of development than mitotic recombination, when there are fewer cells in the eye primordium. Since we do not see many small clones expressing Gal4, this suggests that nearly all eye-antennal disc cells have undergone terminal recombination during embryonic development.

Using CoinFLP-Gal4 to visualize mutant clonal phenotypes

To examine clonal phenotypes using *CoinFLP-Gal4* and *ey-FLP*, crosses were set up as shown in Fig. 2A. To determine if the proportion of Gal4 patches produced is consistent from disc to disc, we first measured the relative area of Gal4-expressing cells in the eye-antennal disc in the absence of a *UAS-RNAi* transgene. Unlike the *Act>y+>Gal4* transgene, which undergoes recombination to express Gal4 in nearly every cell (99%) (Fig. 1I, Fig. 2B), *CoinFLP-Gal4* expresses Gal4 in approximately half of the disc (56%) (Fig. 1D, Fig. 2B,C). A variety of loss-of-function mutations have been described previously that elicit different phenotypes in clones generated by FLP/*FRT*-mediated mitotic recombination when compared with those observed in homozygotes. We tested whether some of these phenotypes could be observed in the adult eye using *CoinFLP-Gal4* with *ey-FLP* and *UAS-RNAi* lines. We included *UAS-dcr2* to increase the efficacy of RNAi (Dietzl et al., 2007). Knockdown of *expanded* (*ex*) (Boedigheimer and Laughon, 1993), a negative regulator of growth, in clones clearly demonstrates the growth advantage exhibited by mutant cells over wild-type cells (Fig. 2B,F,G), whereas uniform *ex* knockdown produces an eye similar in size to that of the wild type (Fig. 2H), although the head capsule is larger (not shown).

Clones of cells heterozygous for mutations in a number of different genes encoding ribosomal proteins (*Minute*) are eliminated in mosaic imaginal discs by a mechanism known as cell competition (Morata and Ripoll, 1975). By contrast, animals that are entirely *Minute* develop to the adult stage. Similarly, using *CoinFLP-Gal4*, patches of cells expressing an RNAi that

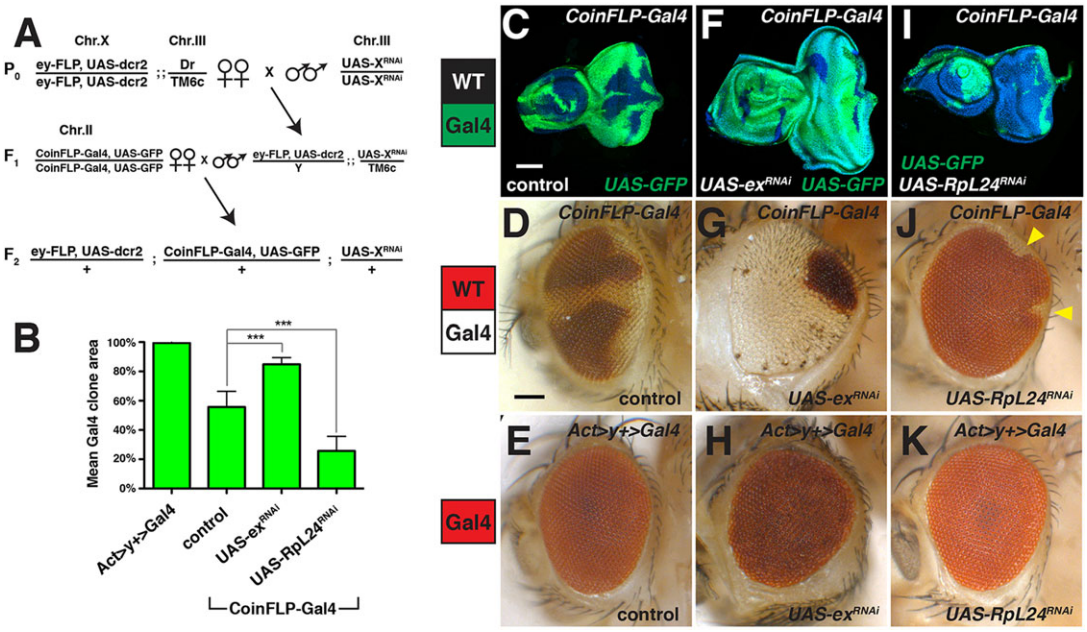

Fig. 2. *CoinFLP-Gal4* mutant phenotypes and comparison with uniform expression. All experiments in this figure use *ey-FLP*. (A) Crossing scheme for generating mosaic eye-antennal discs using *ey-FLP*. (B) Quantification of relative Gal4 clone size in eye-antennal discs for the indicated genotypes. *N*=10 discs/genotype; ***P<0.001; error bars indicate s.d.; quantified using one-way ANOVA with Dunnet's test. (C-E) Control eye-antennal discs and adult eyes, (F-H) *UAS-ex*^{RNAi} and (I-K) *UAS-RpL24*^{RNAi}. (C,F,I) Mosaic eye-antennal discs using *CoinFLP-Gal4*, with Gal4 cells marked with *UAS-GFP* (green) and stained with DAPI (blue). (D,G,J) Mosaic adult eyes using *CoinFLP-Gal4*. Gal4-expressing cells are marked with *UAS-white*^{RNAi} (white). Arrowheads in J indicate *RpL24*^{RNAi} patches remaining in the posterior of the eye. (E,H,K) Adult eyes with *Act>y+>Gal4* and uniform expression of Gal4. Note that these do not include *UAS-white*^{RNAi} and thus eyes have normal red pigment. Eye-antennal discs and adult eyes are positioned with anterior to the left. Genotypes: (C,F,I) *ey-FLP UAS-dcr2/+; CoinFLP-Gal4 UAS-GFP/+; UAS-X/+*; (D,G,J) *ey-FLP UAS-dcr2/+; CoinFLP-Gal4/+; UAS-white*^{RNAi}*/UAS-X*; (E,H,K) *ey-FLP UAS-dcr2/+; Act>y+>Gal4 UAS-GFP/+; UAS-X/+*. Scale bars: 100 µm.

Development (2015) 142, 597-606 doi:10.1242/dev.114603

targets *RpL24*, a likely *Minute* gene (Marygold et al., 2007), are underrepresented in the eye-antennal disc (Fig. 2B,I) and are eliminated from the adult eye (Fig. 2J), except sometimes at the posterior margin where cell proliferation ceases at an earlier stage of development. By contrast, knockdown of *RpL24* in all the cells of the eye has no apparent effect on cell viability (Fig. 2K), demonstrating that these cells are eliminated only when neighboring wild-type cells are present. Another mutation that causes cells to be eliminated by wild-type cells affects the gene *scribble* (*scrib*) (Bilder and Perrimon, 2000). As expected, knockdown of *scrib* in clones results in the elimination of mutant cells (supplementary material Fig. S2C), whereas uniform knockdown results in lethality during development (supplementary material Fig. S2D), which is likely to be due to continued cell proliferation of the eye-antennal discs.

Another advantage of the CoinFLP-Gal4 system over FLP/*FRT*-induced mitotic recombination is that it allows the examination of phenotypes elicited by the overexpression of genes in clones. Overexpression of *reaper* (*rpr*) (White et al., 1994), a pro-apoptotic gene, in clones demonstrates that mutant cells are eliminated while the surviving cells are able to generate an adult eye of normal shape and size (supplementary material Fig. S2E). By contrast, *rpr* overexpression in the entire eye-antennal disc ablates the head (supplementary material Fig. S2F). Overexpression of *Myc* (*diminutive* – FlyBase), a transcription factor, in clones dramatically increases the relative representation of Gal4-positive tissue (supplementary material Fig. S2G), consistent with the ability of Myc to promote growth in a cell-autonomous fashion (Johnston et al., 1999) and to inhibit the survival of neighboring cells that contain lower levels of Myc (de la Cova et al., 2004; Moreno and Basler, 2004). Myc overexpression uniformly in the eye results in a slight overgrowth phenotype (supplementary material Fig. S2H).

Importantly, we find that the CoinFLP-Gal4 system can reveal mutant phenotypes in somatic mosaics that can differ from those observed under conditions of uniform expression. Also, in some cases these phenotypes cannot be visualized under conditions of uniform expression, especially when it results in lethality at an earlier stage of development. Additionally, CoinFLP can be used to examine mosaic phenotypes both in the context of knockdown and of overexpression and can therefore be used for screens that employ collections of RNAi lines (Dietzl et al., 2007; Ni et al., 2011) or collections of cDNAs expressed under *UAS* control (Bischof et al., 2013).

Using CoinFLP-Gal4 for screens: a screen of genes refractory to FLP/*FRT*-mediated mitotic recombination

Screens using FLP/*FRT*-induced mitotic recombination are unable to recover mutations in genes that are located proximal to the *FRT* sites, as well as genes on the fourth and Y chromosomes (supplementary material Fig. S3A). In order to assess the potential of CoinFLP for identifying new genetic pathways involved in cell-cell interactions, we built a *CoinFLP-Gal4* tester stock that contains *ey-FLP* and *UAS-white*^{RNAi}, and set up crosses with 234 *UAS-RNAi* stocks corresponding to 175 genes (Fig. 3A; supplementary material Fig. S3A, Table S2). In parallel, we compared the effects of uniform knockdown in a different tissue by expressing each *UAS-RNAi* in the developing wing pouch with *nubbin-Gal4* (*nb-Gal4*) (supplementary material Table S2).

We observed eye abnormalities in 57 of 234 stocks screened (24%) (Fig. 3B; supplementary material Table S2). Among the genes that scored positive in the screen was *cubitus interruptus* (*ci*) (Orenic et al., 1990), which caused overgrowth especially in the anterior part of the eye (Fig. 3E). Signaling mediated by Smoothened (Smo) is known to inhibit the conversion of Ci from its active to repressive form. Knockdown of *smo*, which would be expected to increase levels of the repressive form of Ci, causes reduced growth (supplementary material Fig. S3B), suggesting that loss of the repressive Ci form is responsible for the overgrowth observed in *ci* mosaics. Knockdown of *shaven* (*sv*) (Fu et al., 1998) caused a reduction in the relative representation of mutant tissue, as well as abnormalities in patterning as assessed by irregularities in the arrangement of mutant ommatidia (Fig. 3F). Knockdown of *pleiohomeotic* (*pho*), a member of the Polycomb group of genes (Simon et al., 1992), resulted in a decrease in the representation of mutant tissue but also caused the partial transformation of antennae to legs (Fig. 3G).

Thirty-seven lines had no, or very small numbers, of mutant cells left in the adult eye, consistent with their elimination at some point in development. When expressed uniformly in the eye, the majority of these lines caused lethality or small eyes/heads (Fig. 3C), suggesting that these genes are necessary for cell proliferation or viability. For example, clones with reduced *rolled* (*rl*) function, which is the *Drosophila* ortholog of MAP kinase (Biggs et al., 1994), were absent and the overall size of the eye was reduced (Fig. 3H). Uniform knockdown of *rl* results in near-complete loss of the eye (Fig. 3K). This contrasts dramatically with the phenotypes elicited by knockdown of *geminin*, which encodes a regulator of the initiation of DNA replication (Quinn et al., 2001). Knockdown of *geminin* in clones resulted in the complete elimination of mutant cells (Fig. 3I; supplementary material Fig. S3C,D). However, uniform knockdown had no effect on the size or morphology of the adult eye or head (Fig. 3L). This suggests that *geminin*^{RNAi} cells are predisposed to elimination only in the presence of wild-type tissue, which is a characteristic of the phenomenon of cell competition (Morata and Ripoll, 1975). Additionally, uniform knockdown of *geminin* in the wing (supplementary material Fig. S3E,F) or ubiquitously (Fig. 3N) does not cause obvious morphological or size defects (supplementary material Fig. S3E). Three additional independent *geminin*^{RNAi} lines gave the same elimination phenotype when expressed in mosaic eyes, yet caused varying degrees of cell lethality when uniformly expressed in the eye, wing, or ubiquitously (supplementary material Fig. S3F), indicating that there might be a threshold above which more *geminin* knockdown causes autonomous cell viability defects. Thus, the CoinFLP-Gal4 system can identify novel regulators of cell competition.

CoinFLP-LexGAD/Gal4: a system for expressing two different genes in subpopulations of clones

The CoinFLP-Gal4 system enables the expression of RNAi constructs or cDNAs in subsets of clones. This allows the study of interactions between mutant clones and wild-type cells. However, to enable the study of interactions between two different types of mutant cells we developed a second system, CoinFLP-LexGAD/Gal4 (Fig. 4A). In this system, FLP recombination of canonical *FRT* sites results in excision of the STOP cassette and expression of the transcriptional activator LexGAD (Lai and Lee, 2006; Szuts and Bienz, 2000), which can activate the expression of genes that are downstream of the *LexA* operator (*LexAop*). Recombination between *FRT3* sites excises both the STOP cassette and the *LexGAD* gene, resulting in the expression of Gal4. This results in the generation of mosaic tissue in which some patches express Gal4 and others express LexGAD.

Development (2015) 142, 597-606 doi:10.1242/dev.114603

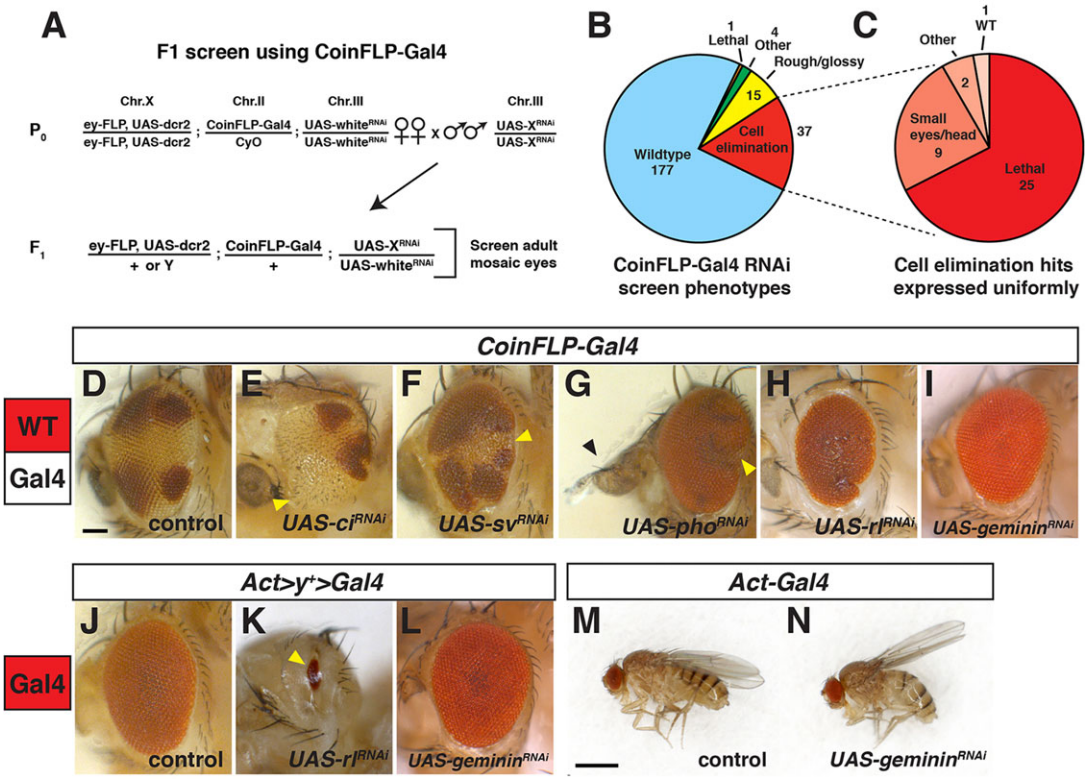

Fig. 3. *CoinFLP-Gal4* RNAi screen for phenotypic abnormalities in mosaic eyes. All experiments in this figure, except M and N, use *ey-FLP*. (A) Crossing scheme showing the *CoinFLP-Gal4* tester stock. (B) Summary of phenotypes observed in the screen. (C) Secondary screen to test cell elimination RNAi hits under conditions of uniform expression. The pie charts show the number of different phenotypes. (D-I) Adult eyes, showing examples of phenotypes obtained under conditions of mosaic Gal4 expression in the eye with *CoinFLP-Gal4* (as discussed in the main text). Yellow arrowheads point to white mutant tissue. Black arrowhead points to antenna-to-leg transformation. (I) *UAS-geminin*^{RNAi} cells are eliminated from the mosaic eye. (J-L) Adult eyes, showing examples of phenotypes obtained under conditions of uniform Gal4 expression in the eye using *Act>y+>Gal4* (as discussed in the main text). Yellow arrowhead indicates a small amount of remaining eye tissue from *UAS-rl*^{RNAi} expression. (L) *UAS-geminin*^{RNAi} eyes are morphologically normal. Note that these do not include *UAS-white*^{RNAi} and thus eyes have normal red pigment. (M,N) Adult flies with ubiquitous expression of *Act-Gal4*. Control (M) and *UAS-geminin*^{RNAi} (N) flies are viable and similar in size. Adult eyes and flies are positioned with anterior to the left. Genotypes: (D-I) *ey-FLP UAS-dcr2/+; CoinFLP-Gal4/+; UAS-white*^{RNAi}*/UAS-X*; (J-L) *ey-FLP UAS-dcr2/+; Act>y+>Gal4 UAS-GFP/+; UAS-X/+*; (M,N) *UAS-dcr2/+; Act-Gal4/+; UAS-X/+*. Scale bars: 100 µm in D-L; 1 mm in M,N.

Fluorescent reporters such as *UAS-RFP* and *LexAop-GFP* can separately mark the Gal4-expressing and LexGAD-expressing cells. When *ey-FLP* was used (crossing scheme in Fig. 4B), both Gal4-expressing and LexGAD-expressing clones were generated in the eye-antennal disc (Fig. 4C). As expected, clonal boundaries sometimes fell within individual ommatidia (Fig. 4C′) (Ready et al., 1976), generating ommatidia in which some cells expressed LexGAD while others expressed Gal4. If no recombination had occurred, the cells would express neither Gal4 nor LexGAD. Such clones were rare in the eye-antennal disc (Fig. 4C,C′) and the adult eye (supplementary material Fig. S4A-A″). When *senseless* (*sens*)-*FLP* was used, which is expressed in R8 photoreceptors (Chen et al., 2014), single cells expressed either Gal4 or LexGAD (Fig. 4D,D′). A number of Sens-positive cells expressed neither Gal4 nor LexGAD (Fig. 4D′). Interestingly, immediately posterior to the morphogenetic furrow, where Sens is first expressed, R8 cells do not express Gal4 or LexGAD. In more posterior rows of R8 cells, both Gal4-expressing and LexGAD-expressing cells are observed, indicating that the probability of conversion to a Gal4-expressing or LexGAD-expressing state increases with time of FLP expression. This contrasts with the almost complete conversion observed in the third instar disc with *ey-FLP*, which might be the result of higher expression levels than *sens-FLP*. Alternatively, because *ey* is expressed in the embryonic precursor cells of the eye before the onset of their proliferation in the larva, complete conversion might have occurred before proliferation begins. We also found rare cells expressing Gal4 or LexGAD that do not express Sens, immediately adjacent to Sens-expressing cells. These are likely to be cells of the R8 equivalence group, which express Sens transiently before the selection of a single Sens-expressing R8 cell (Frankfort et al., 2001). Using a heat shock-inducible source of FLP (*hs-FLP*), Gal4-expressing and LexGAD-expressing clones were observed in eye-antennal discs (Fig. 4E,E′), as well as patches that expressed neither.

To quantify recombination choice in the *CoinFLP-LexGAD/Gal4* construct, we measured the number of Gal4-expressing and LexGAD-expressing cells in eye-antennal discs using *ey-FLP* and *sens-FLP*. For *ey-FLP*, we measured the areas of clones and found that Gal4-expressing clones are less frequent than LexGAD-expressing clones (19% compared with 80%, respectively; N=20 discs; s.d.=8%) (Fig. 4F). Clones expressing neither represent 1% of the total. For *sens-FLP*, because of ongoing recombination in the larval disc, we only counted the number of cells expressing Gal4 or LexGAD and again found that Gal4 expression was less frequent (8% compared with 92%, respectively; N=1311 cells). One interpretation could be that Gal4 and LexGAD cells are produced in similar quantities initially, but Gal4-expressing cells are disproportionally lost due to the toxicity of Gal4, as previously shown in other contexts (Rezaval et al., 2007). An alternative

Development (2015) 142, 597-606 doi:10.1242/dev.114603

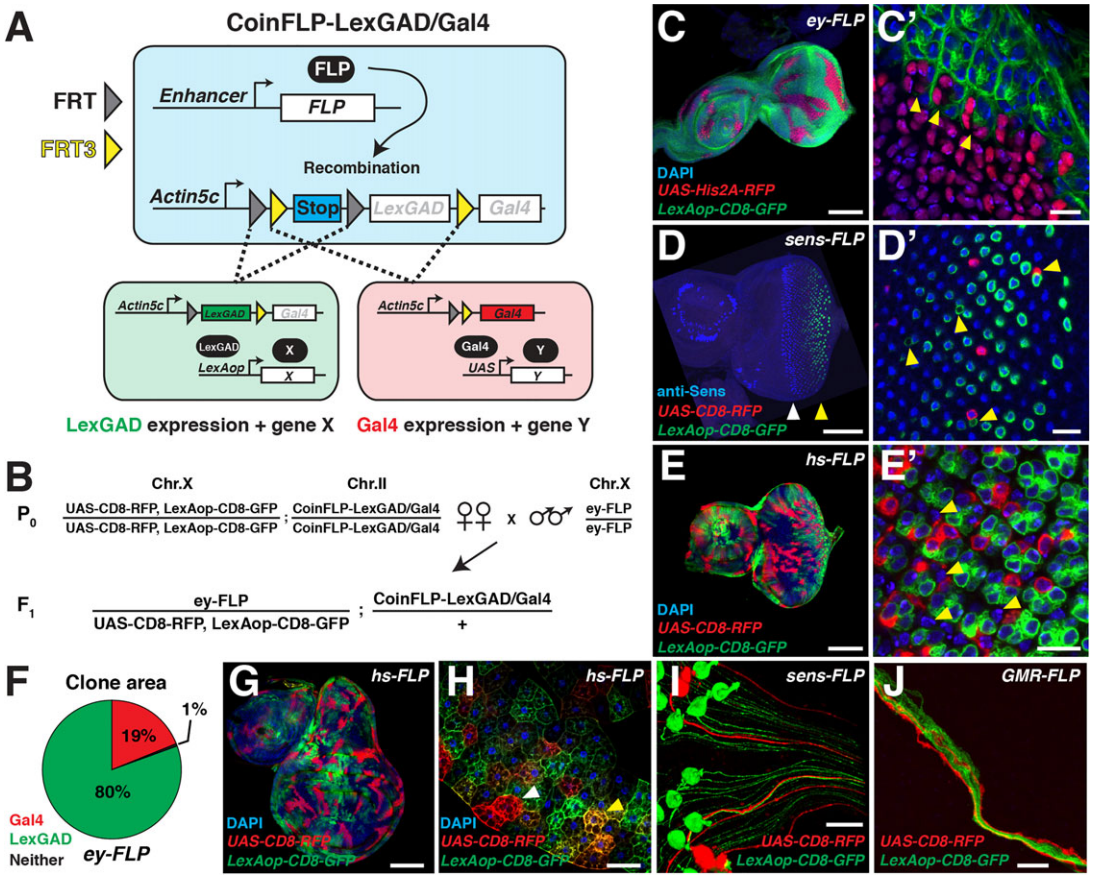

Fig. 4. The CoinFLP-LexGAD/Gal4 system. (A) Recombination between *FRT* sites results in excision of the STOP cassette and expression of LexGAD (green). Recombination between *FRT3* sites results in excision of the STOP cassette and LexGAD and hence expression of Gal4 (red). (B) Crossing scheme for the generation of Gal4-expressing and LexGAD-expressing cells using *ey-FLP*. (C) Confocal slice of an eye-antennal disc with *ey-FLP*-induced expression of LexGAD (green) or Gal4 (red) in clones. DAPI is in blue. (C′) Magnification of C in the posterior of the eye disc; arrowheads indicate mosaic ommatidia. (D) Confocal projection of an eye-antennal disc with *sens-FLP*-induced expression of LexGAD (green) or Gal4 (red) in photoreceptors. Anti-Sens is in blue. White arrowhead indicates first expression of Sens at the morphogenetic furrow; yellow arrowhead indicates that the most recombined and fluorescing cells are more posterior. (D′) Magnification of D in the posterior of the eye disc. Arrowheads point to Gal4-expressing or LexGAD-expressing cells that do not express Sens. (E) Confocal slice of an eye-antennal disc with *hs-FLP*-induced expression of LexGAD (green) or Gal4 (red) in clones. DAPI is in blue. (E′) Magnification of E; arrowheads indicate cells that do not express either LexGAD or Gal4. (F) Quantification of Gal4-expressing and LexGAD-expressing clone areas in eye-antennal discs expressing *ey-FLP*. *n*=20 discs; s.d.=8%; quantification using a one-way ANOVA test. (G) Wing disc with clones that express either LexGAD (green) or Gal4 (red). (H) Fat body with cells that each express different amounts of Gal4 and LexGAD. White arrowhead indicates a cell that is predominantly Gal4 expressing; yellow arrowhead indicates a cell that expresses both Gal4 and LexGAD (yellow). (I) Photoreceptor axons in the eye-antennal disc expressing LexGAD (green) or Gal4 (red), using *sens-FLP*. (J) Axons in the Bolwig nerve expressing LexGAD (green) or Gal4 (red) using *GMR-FLP*. Eye-antennal discs in C,D,E,I are positioned with anterior to the left. Genotypes: (C,C′) *ey-FLP/+; CoinFLP-LexGAD|Gal4/LexAop-CD8-GFP; UAS-His-RFP/+*; (D,D′,I) *sens-FLP/UAS-CD8:RFP, LexAop-CD8:GFP; CoinFLP-LexGAD|Gal4/+*; (E,E′,G,H) *hs-FLP/UAS-CD8:RFP, LexAop-CD8:GFP; CoinFLP-LexGAD|Gal4/+*; (F) *ey-FLP/UAS-CD8:RFP, LexAop-CD8:GFP; CoinFLP-LexGAD|Gal4/+*; (J) *UAS-CD8:RFP, LexAop-CD8:GFP/+; CoinFLP-LexGAD|Gal4/GMR-FLP*. Scale bars: 100 µm in C,D,E,G,H; 10 µm in C′,D′,E′,I,J. Note that *CoinFLP-LexGAD|Gal4* is used in genotypes instead of *CoinFLP-LexGAD/Gal4* where the solidus is used to indicate homologous chromosomes.

interpretation is that the relative recombination efficiency of *FRT* sites is less than for *FRT3* sites in the *CoinFLP-LexGAD/Gal4* construct. Since *FRT* and *FRT3* sites have similar recombination frequencies (Schlake and Bode, 1994), the shorter distance between *FRT*s (411 bp) compared with *FRT3*s (3531 bp) in this construct might explain the difference in the frequency of LexGAD and Gal4 expression. Indeed, *FRT* recombination frequency is known to be reduced with increasing distance (Ringrose et al., 1999).

To demonstrate the wider applicability of the CoinFLP-LexGAD/Gal4 system, we examined other tissues and cell types and tested additional FLP sources. Using *hs-FLP*, we observed cells expressing either LexGAD or Gal4 in virtually every tissue examined at larval and adult stages, such as the wing disc (Fig. 4G; supplementary material Fig. S4B-B‴) and polyploid fat body cells (Fig. 4H; supplementary material Fig. S4C-C‴). Interestingly, in these polyploid cells, co-expression of LexGAD and Gal4 was frequently observed, presumably because the presence of multiple copies of the construct in the same cell allows both *FRT*- and *FRT3*-mediated recombination. We also imaged neurons expressing either LexGAD or Gal4, facilitated by the use of membrane-bound fluorescent markers to visualize fine projections such as axons and dendrites. *sens-FLP* mostly labeled R8 photoreceptors and their axons, which project toward the optic lobe of the larval brain (Fig. 4I), whereas *GMR-FLP* (Chen et al., 2014) labeled axons of the Bolwig nerve (Fig. 4J), and *20C11-FLP* (Chen et al., 2014), which drives FLP from an *Octβ1R* regulatory fragment, labeled a small subset of neurons in the larval brain (supplementary material Fig. S4D). Importantly, whereas previous techniques such as Brainbow have labeled multiple cells with fluorescent markers, the CoinFLP-LexGAD/Gal4 system allows the inclusion of RNAi or overexpression transgenes to affect gene activity in labeled cells.

Development (2015) 142, 597-606 doi:10.1242/dev.114603

Visualizing clonal boundaries by combining CoinFLP-LexGAD/Gal4 with GRASP

The CoinFLP-LexGAD/Gal4 system also allows the visualization of clonal boundaries by combining it with the GFP reconstitution across synaptic partners (GRASP) system (Feinberg et al., 2008; Gordon and Scott, 2009). In the GRASP system, two complementary parts of a 'split GFP' (spGFP1-10 and spGFP11) are fused to the extracellular domains of mouse CD4, one under *UAS* control and the other under *LexAop* control. Thus, the two components can reconstitute GFP at the boundaries where LexGAD-expressing cells contact Gal4-expressing cells (Fig. 5A). We illustrated the utility of the system in visualizing follicle cell clones in adult ovaries. Using *hs-FLP*, we generated mosaic egg chambers that expressed patches of Gal4 and LexGAD (crossing scheme in Fig. 5B). Most egg chambers are composed of the progeny of two follicle cell stem cells (Nystul and Spradling, 2010). However, in the example shown in Fig. 5C, we observed a stage 9 egg chamber that is likely to consist of three clones: two that express either Gal4 or LexGAD and a third that expresses neither. As predicted, GFP fluorescence was mostly observed at the interface between LexGAD-expressing cells and Gal4-expressing cells (Fig. 5C,C′). Interestingly, a low level of punctate GFP expression was observed far from the boundary, especially in the part of the egg chamber that expresses

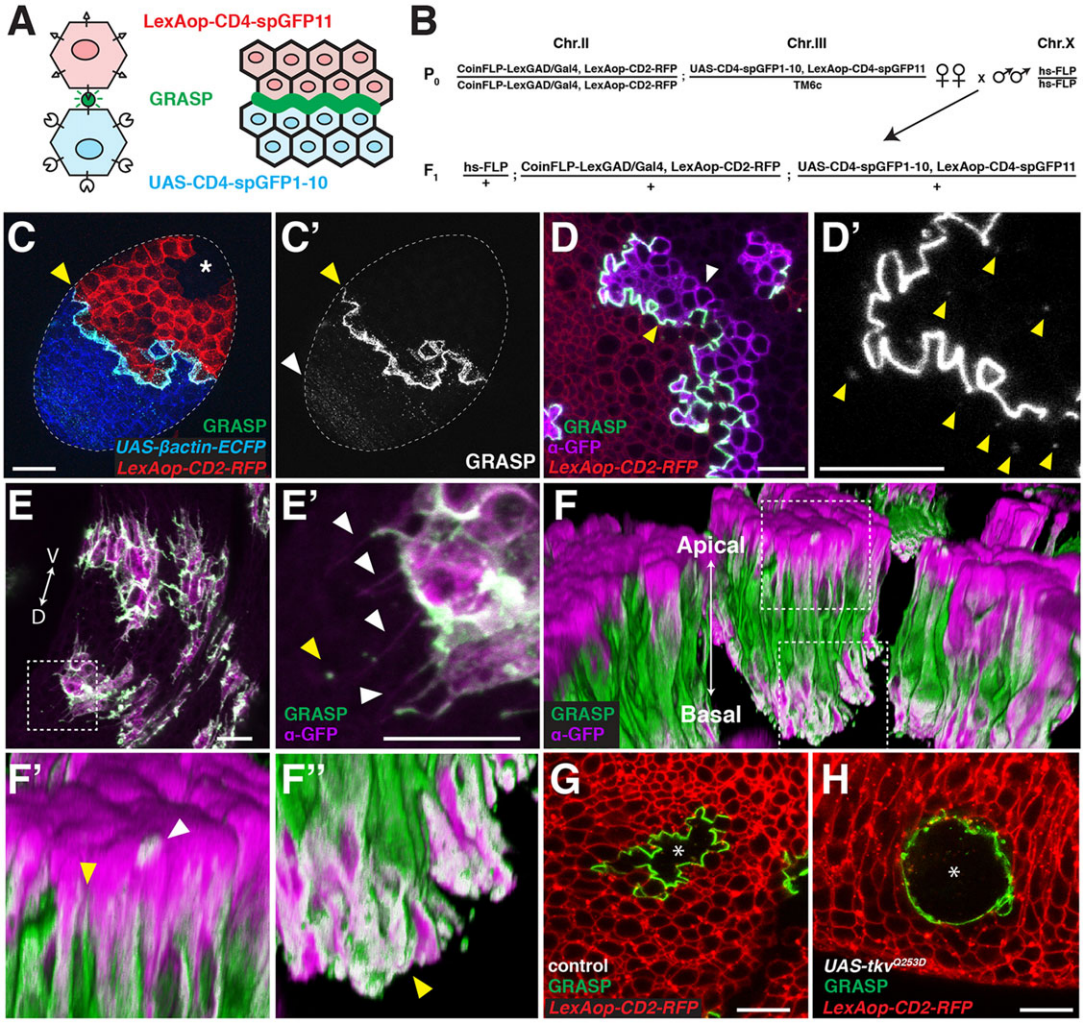

Fig. 5. Visualizing cellular contacts using GRASP. (A) GRASP fluorescence marks the boundary between two clones that express either CD4-spGFP1-10 or CD4-spGFP-11. (B) Crossing scheme for generation of GRASP-marked cell boundaries using *hs-FLP*. (C,C′) Confocal projection of an egg chamber composed of follicle cells that express LexGAD (red), Gal4 (blue) or neither (asterisk), induced with *hs-FLP*. GRASP fluorescence (green) labels the boundary between LexGAD-expressing cells and Gal4-expressing cells (yellow arrowhead). White arrowhead shows puncta arranged in a circumferential belt. (D-H) Wing imaginal discs with *hs-FLP*-induced clones and GRASP (green). (D) A confocal section midway through the epithelium of the wing disc proper. GRASP outlines the boundaries (yellow arrowhead) between cells expressing LexGAD (red) and Gal4 (magenta). Gal4-expressing cells are labeled with anti-GFP (magenta), which recognizes spGFP1-10; white arrowhead indicates boundary between Gal4-expressing cells and wild-type cells that lack GRASP. (D′) Higher magnification of D. Arrowheads indicate punctate fluorescence away from the boundary. (E) Confocal projection showing basal processes emerging from the clone boundary. Double-headed arrow indicates the dorsoventral axis. (E′) Higher magnification of E. Basal processes (white arrowheads) have puncta of GRASP at their tip (yellow arrowhead). (F) 3D projection of GRASP-labeled contact between clonal boundaries. Apicobasal cell polarity is indicated. (F′,F″) Higher magnification of F showing (F′) apical contact with overlying peripodial membrane (white arrowhead) and apical contact boundary with neighboring disc cells (yellow arrowhead), and (F″) the basal contact boundary (arrowhead). (G,H) Confocal slice through a wing disc clone with GRASP fluorescence (green) at the boundary. Asterisk marks Gal4-expressing cells. (G) Control, (H) *UAS-tkv*^{Q253D}. All panels have *UAS-CD4-spGFP1-10* and *LexAop-CD4-spGFP11*. Genotypes: (C,C′) *hs-FLP/+; CoinFLP-LexGAD|Gal4 LexAop-CD2-RFP/UAS-CFP-actin; UAS-CD4-spGFP1-10, LexAop-CD4-spGFP11/+*; (D-G) *hs-FLP/+; CoinFLP-LexGAD|Gal4, LexAop-CD2-RFP/+; UAS-CD4-spGFP1-10, LexAop-CD4-spGFP11/+*; (H) *hs-FLP/+; CoinFLP-LexGAD|Gal4, LexAop-CD2-RFP/UAS-tkv*^{Q253D}*; UAS-CD4-spGFP1-10, LexAop-CD4-spGFP11/+*. Scale bars: 10 µm.

Development (2015) 142, 597-606 doi:10.1242/dev.114603

UAS-spGFP1-10 (Fig. 5C′). The reason for this is unclear, although the puncta were aligned in circumferential bands that would be consistent with their secretion into the basement membrane by follicle cells that are crawling circumferentially around the egg chamber (Haigo and Bilder, 2011).

We also visualized clonal boundaries in the wing imaginal disc using GRASP. When clones were generated with *hs-FLP*, we observed both LexGAD-expressing and Gal4-expressing cells, as well as GFP fluorescence at the boundaries between them (Fig. 5D-F″). In a confocal section midway between the apical and basal surfaces of the disc epithelial cells, GFP was observed at the clonal boundary as well as in puncta on both sides of the boundary (Fig. 5D,D′). These puncta might be the contacts of lateral protrusions (Demontis and Dahmann, 2007). Reconstructed confocal sections of the basal surface (Fig. 5E,E′) revealed thin processes reminiscent of cytonemes (Hsiung et al., 2005), which were observed emanating from the clonal boundary and aligned with the dorsoventral axis (Fig. 5E). GFP puncta were sometimes observed at the tip of these processes (Fig. 5E′), suggesting that they make more stable contacts at their endpoints. A 3D reconstruction shows the extent of cell-cell contact along the lateral surface of wing disc cells (Fig. 5F-F″; supplementary material Movie 1). Surprisingly, these images reveal less cell-cell contact near the apical surface as compared with the basal surface (Fig. 5F′,F″). Furthermore, we observed points of contact between the apical membrane of cells in the disc proper and the overlying peripodial membrane (Fig. 5F′) (Demontis and Dahmann, 2007).

Many genetic changes are known to cause mutant clones to adopt rounder shapes, presumably because of altered adhesion between mutant and wild-type cells. For example, activation of Dpp signaling through the Thickveins (Tkv) receptor causes increased growth of cells and smoother clonal boundaries with wild-type cells (Martin-Castellanos and Edgar, 2002). Using GRASP, we find that, whereas wild-type clones have irregular boundaries (Fig. 5G), clones expressing an activated Tkv receptor (Tkv^{Q253D}) have smooth boundaries (Fig. 5H). Thus, the CoinFLP-LexGAD/Gal4 system together with GRASP can be used to visualize boundaries and regions of cell-cell contact between genetically distinct populations of cells.

DISCUSSION

The CoinFLP-Gal4 system facilitates mosaic Gal4/*UAS* screens by automatically generating mosaic tissue in a developmentally restricted manner. We have used this system to perform a pilot RNAi screen, focusing on genes that are refractory to traditional mosaic analysis. We identified several mutant phenotypes, one of which, induced by $geminin^{RNAi}$, appears to cause mutant cells to be eliminated by cell competition. *geminin* has not been previously implicated in cell competition and therefore deserves further study. Importantly, this phenotype could only be identified in the context of a mosaic environment, suggesting that the CoinFLP-Gal4 system can be used for larger scale screens to find novel regulators of cell-cell interactions.

Many of the shortcomings of mutagenesis-based genetic screens have been overcome by screens that use RNAi. There are collections of fly stocks available that target most, if not all, annotated genes (Dietzl et al., 2007; Ni et al., 2011). With RNAi screens, the identity of the gene is known from the outset, thus saving the effort required for gene identification by mapping and/or genome sequencing. Additionally, targeting the expression of these RNAi transgenes to a specific tissue (e.g. the eye) overcomes any requirement for the genes being tested at earlier stages of development or in all tissues. However, until now, it was not easy to conduct mosaic screens using RNAi in which a reliable ratio of wild-type and mutant cells is consistently achieved, such that deviations from the normal ratio can be easily scored. Additionally, CoinFLP-Gal4 can be used to screen mosaic phenotypes associated with the overexpression of genes using collections of cDNAs expressed under the control of *UAS* elements (Bischof et al., 2013).

The CoinFLP-LexGAD/Gal4 system allows the control of gene expression in two different populations within the same tissue. For example, this technique can be used to generate different labeled mutant clones and observe their interaction. In addition, we have used this system with GRASP to visualize clonal boundaries in the egg chamber and wing imaginal disc, especially the surfaces between adjacent cells and other points of contact (e.g. along processes). There is some controversy as to whether GRASP increases the affinity of cell-cell interactions (Feinberg et al., 2008; Kim et al., 2012). It is likely that future versions of GRASP will address some of these possible shortcomings. The generation of other split proteins that can be reconstituted to provide an activity that can be scored in adult tissues might further enhance the ability to use *CoinFLP-LexGAD/Gal4* in live undissected flies. Finally, *CoinFLP-LexGAD/Gal4* could be used to perform more elaborate mosaic screens to study cell-cell interactions, where gene activity is altered in one population of cells while the other cell population is systematically screened by RNAi or overexpression libraries.

In its present form, the CoinFLP system is useful for inducing Gal4 or LexGAD expression from a constitutive promoter in mosaic patches in a specific tissue. However, further modifications to this system can be made. For example, instead of the *Actin 5C* promoter, a tissue-specific promoter could be used to help spatially restrict gene expression. Similarly, different tissue-specific sources of FLP can be used to restrict mosaicism to a desired cell lineage. Furthermore, other genes can be used in place of *Gal4* or *LexGAD*, such as *QF*, which drives genes under *QUAS* control (Potter et al., 2010). Also, different arrangements of variant *FRT* sites can be used, such as employed in the FlEx system (Schnutgen et al., 2005), or additional variant *FRT* sites such as *FRT5* (Schlake and Bode, 1994) can be added to increase the number of unique mosaic patches. Finally, one can manipulate the relative quantity of Gal4-expressing and LexGAD-expressing cells by swapping the two coding sequences, such that Gal4 may then be more frequent than LexGAD, or by changing the distance between *FRT* sites.

MATERIALS AND METHODS

Construction of the CoinFLP systems

Detailed descriptions of how the CoinFLP systems were constructed are provided in the supplementary Materials and Methods, including plasmid maps of *CoinFLP-Gal4* (supplementary material Fig. S5) and *CoinFLP-LexGAD/Gal4* (supplementary material Fig. S6).

Fly genetics

All crosses were maintained at 25°C on standard fly medium (BDSC) supplemented with yeast pellets. Most fly lines used are available from the Bloomington *Drosophila* Stock Center at Indiana University (BL) unless otherwise noted. Fly lines used: *ey-FLP* (X, BL5580), *Ubx-FLP* (BL42718), $UAS\text{-}white^{RNAi}$ (III, BL33623), *Act>y+>Gal4* (II, BL3953), *UAS-EGFP* (II, BL6874), *UAS-dcr2* (X, BL24646), *40AFRT* (Xu and Rubin, 1993), *ey-FLP; 40AFRT ubi-GFP* (derived from BL5189), $UAS\text{-}RpL24^{RNAi}$ (BL34569), $UAS\text{-}ex^{RNAi}$ (BL28703), *y v; attP2* (negative control for TRiP stocks, BL36303), *UAS-dcr2; nb-Gal4* (BL25754), *UAS-dcr2; Act-Gal4* (BL25708), *UAS-ECFP-β-actin* (BL7064), *10XUAS-IVS-mCD8::RFP, 13XLexAop2-mCD8::GFP* (BL32229), *LexAop-rCD2::RFP* (II) (Awasaki et al., 2011), *LexAop-rCD2::GFP* (Lai and Lee, 2006), *UAS-His2A-RFP* (III) (Emery et al., 2005), *UAS-CD4::spGFP1-10* (III),

Development (2015) 142, 597-606 doi:10.1242/dev.114603

LexAop-CD4::spGFP11 (III) (Gordon and Scott, 2009), *UAS-ci*^{RNAi} (BL28984), *UAS-sv*^{RNAi} (BL27269), *UAS-pho*^{RNAi} (BL31609), *UAS-rl*^{RNAi} (BL34855), *UAS-geminin*^{RNAi} (GLV21038, BL35673, used in Fig. 3), *sens-FLP* (BL55768), *GMR-FLP* (Chen et al., 2014), *UAS-tkv*^{Q253D} (BL36536), *UAS-ebony*^{RNAi} (BL28612), *UAS-forked*^{RNAi} (BL41687), *UAS-mwh*^{RNAi} (BL34862), *UAS-scrib*^{RNAi} (VDRC 27424), *UAS-rpr* (BL5824), *UAS-myc* (Johnston et al., 1999), *UAS-smo*^{RNAi} (BL53348), *20C11-FLP* (BL55766).

Stocks used in experiments shown in the supplementary material that are not described in main text: *UAS-geminin*^{RNAi} GL01299 (BL41869), *UAS-geminin*^{RNAi} (BL30929), *UAS-geminin*^{RNAi} HMS02954 (BL50720). *ey-FLP* stocks used are listed in supplementary material Table S1 and *UAS-RNAi* stocks used are listed in supplementary material Table S2. Supplementary material Table S3 includes descriptions of CoinFLP stocks deposited at the Bloomington *Drosophila* Stock Center. Information on how we selected the RNAi lines for the CoinFLP-Gal4 screen is described in the supplementary Materials and Methods.

To aid in testing multiple *UAS* lines by genetic crosses, such as conducting a genetic screen, we generated a 'tester' fly stock that contains several transgenes to produce mosaic adult eyes with *white*^{RNAi} marking Gal4 patches: *ey-FLP, UAS-dcr2; CoinFLP-Gal4 attP40; UAS-white*^{RNAi}. This tester stock breaks down relatively often and we therefore recommend that this stock is constructed each time from stocks that we have deposited in the Bloomington *Drosophila* Stock Center. Additionally, as a comparison for mosaic Gal4 expression, we constructed an analogous tester stock that induces uniform expression of Gal4 from the *Actin 5C* promoter in most, if not all, eye-antennal disc cells following FLP-induced excision of a STOP cassette: *ey-FLP, UAS-dcr2; Act>y+>Gal4 UAS-GFP.*

Dissections, immunohistochemistry and microscopy

Imaginal discs were dissected from wandering third instar larvae, or ovaries were dissected from adult flies, fixed in 4% paraformaldehyde for 20 min, and washed with PBS. Samples were incubated in DAPI and mounted on slides with SlowFade Gold mounting medium (Life Technologies). Fixed samples processed for antibody staining were permeabilized in PBS+0.1% Triton-X100 for 20 min, blocked with PBS+0.1% Triton-X100+5% normal goat serum for 1 h, and incubated with primary antibodies diluted in blocking solution overnight at 4°C. Samples were washed three times for 15 min each in PBS+0.1% Triton-X100. Samples were incubated with secondary antibodies and washed as for primary antibodies. Mounted samples were imaged on a Zeiss 700 confocal microscope. Confocal slices were processed with ImageJ software (NIH). Confocal stacks were processed with Volocity software (Perkin Elmer) to generate 3D projections.

Staining reagents: guinea pig anti-Sens (1:500; H. Bellen, Baylor College, Houston, USA); rabbit anti-GFP (1:800; Abcam ab290), which recognizes spGFP1-10 and reconstituted spGFP, but not spGFP11 (Gordon and Scott, 2009); 1 ng/µl DAPI.

For experiments requiring heat shock induction of the *hs-FLP* transgene in larvae, 48 h after egg deposition (AED) larvae were placed in a 37°C water bath for 30 min. Larvae were dissected as wandering third instar larvae at 120 h AED. For heat shock induction in follicle cells, adult female flies were heat shocked for 10 min and ovaries were dissected 2 days later.

Imaging adult flies and quantification of mosaic eyes

Adult female flies were frozen overnight and eyes were imaged on a Leica transmitted light microscope (TL RCI) at identical settings. White versus red ratios in mosaic eyes were determined by measuring the area (pixels^2) of red eye tissue in Photoshop CS6 (Adobe) and comparing with the total area of the eye. To image fluorescence in adult eyes, flies were sedated with CO_2 and Flynap (173010, Carolina) and fluorescence was imaged using a Zeiss stereo microscope (Lumar.V12).

Quantification of wing size

Wings were mounted onto slides using Canadian Balsam medium (Gary's Magic Mount) and imaged on a Leica TL RCI. Wing area was measured in ImageJ using the polygon selection tool. Statistical significance between groups was determined by one-way ANOVA using Tukey's test. At least 30 wings/genotype were used.

Quantification of clone size and cell number

Confocal images of eye-antennal discs were processed using ImageJ. Clone area and total disc size were measured using the polygon selection tool. Cell number was measured using the multi-point selection tool. Statistical significance between groups was determined by one-way ANOVA using Tukey's test. For quantifications of *CoinFLP-Gal4* recombination with *ey-FLP*, ten eye-antennal discs were used for each genotype (*ey-FLP UAS-dcr2/+; CoinFLP-Gal4 UAS-GFP/+; UAS-X/+*). For quantifications of *CoinFLP-LexGAD/Gal4* with *ey-FLP*, 20 eye-antennal discs were used (genotype: *ey-FLP/UAS-CD8-RFP, LexAop-CD8-GFP; CoinFLP-LexGAD|Gal4/+*). For quantifications of *CoinFLP-LexGAD/Gal4* with *sens-FLP*, 1311 cells were counted (genotype: *sens-FLP/UAS-CD8-RFP, LexAop-CD8-GFP; CoinFLP-LexGAD|Gal4/+*).

Acknowledgements

We thank Taryn Sumabat for discussions; Joanna Downes for help with plasmid constructions; Cassandra Van and Geoffrey Logan for experimental assistance; Laura Johnston, Tzumin Lee, Duojia Pan and Kristin Scott for fly stocks; Gerry Rubin, David Strutt and Larry Zipursky for plasmids; and Joelle Lomax for suggesting the name 'CoinFLP'.

Competing interests

The authors declare no competing or financial interests.

Author contributions

J.A.B. designed and built the CoinFLP system. J.A.B. and I.K.H. designed and interpreted experiments. J.A.B. conducted most experiments. N.H.T. conducted part of the genetic screen. J.A.B. prepared the figures. J.A.B. and I.K.H. wrote the paper.

Funding

This work was supported by grants [R01GM61672 and R21EY23924] from the National Institutes of Health and an American Cancer Society Research Professor Award [120366-RP-11-078-01-DDC] to I.K.H. J.A.B. was funded by a National Science Foundation Graduate Research Fellowship and then a fellowship from the Cancer Research Coordinating Committee of the University of California. Deposited in PMC for release after 12 months.

Supplementary material

Supplementary material available online at
http://dev.biologists.org/lookup/suppl/doi:10.1242/dev.114603/-/DC1

References

Awasaki, T., Huang, Y., O'Connor, M. B. and Lee, T. (2011). Glia instruct developmental neuronal remodeling through TGF-beta signaling. *Nat. Neurosci.* **14**, 821-823.

Benlali, A., Draskovic, I., Hazelett, D. J. and Treisman, J. E. (2000). act up controls actin polymerization to alter cell shape and restrict Hedgehog signaling in the *Drosophila* eye disc. *Cell* **101**, 271-281.

Biggs, W. H., III, Zavitz, K. H., Dickson, B., van der Straten, A., Brunner, D., Hafen, E. and Zipursky, S. L. (1994). The *Drosophila* rolled locus encodes a MAP kinase required in the sevenless signal transduction pathway. *EMBO J.* **13**, 1628-1635.

Bilder, D. and Perrimon, N. (2000). Localization of apical epithelial determinants by the basolateral PDZ protein Scribble. *Nature* **403**, 676-680.

Bischof, J., Bjorklund, M., Furger, E., Schertel, C., Taipale, J. and Basler, K. (2013). A versatile platform for creating a comprehensive UAS-ORFeome library in *Drosophila*. *Development* **140**, 2434-2442.

Boedigheimer, M. and Laughon, A. (1993). Expanded: a gene involved in the control of cell proliferation in imaginal discs. *Development* **118**, 1291-1301.

Brand, A. H. and Perrimon, N. (1993). Targeted gene expression as a means of altering cell fates and generating dominant phenotypes. *Development* **118**, 401-415.

Cai, D., Cohen, K. B., Luo, T., Lichtman, J. W. and Sanes, J. R. (2013). Improved tools for the Brainbow toolbox. *Nat. Methods* **10**, 540-547.

Chen, Y., Akin, O., Nern, A., Tsui, C. Y. K., Pecot, M. Y. and Zipursky, S. L. (2014). Cell-type-specific labeling of synapses in vivo through synaptic tagging with recombination. *Neuron* **81**, 280-293.

Clavería, C., Giovinazzo, G., Sierra, R. and Torres, M. (2013). Myc-driven endogenous cell competition in the early mammalian embryo. *Nature* **500**, 39-44.

Colombani, J., Andersen, D. S. and Leopold, P. (2012). Secreted peptide Dilp8 coordinates *Drosophila* tissue growth with developmental timing. *Science* **336**, 582-585.

de la Cova, C., Abril, M., Bellosta, P., Gallant, P. and Johnston, L. A. (2004). *Drosophila* myc regulates organ size by inducing cell competition. *Cell* **117**, 107-116.
Demontis, F. and Dahmann, C. (2007). Apical and lateral cell protrusions interconnect epithelial cells in live *Drosophila* wing imaginal discs. *Dev. Dyn.* **236**, 3408-3418.
Dietzl, G., Chen, D., Schnorrer, F., Su, K.-C., Barinova, Y., Fellner, M., Gasser, B., Kinsey, K., Oppel, S., Scheiblauer, S. et al. (2007). A genome-wide transgenic RNAi library for conditional gene inactivation in *Drosophila*. *Nature* **448**, 151-156.
Emery, G., Hutterer, A., Berdnik, D., Mayer, B., Wirtz-Peitz, F., Gaitan, M. G. and Knoblich, J. A. (2005). Asymmetric Rab11 endosomes regulate delta recycling and specify cell fate in the *Drosophila* nervous system. *Cell* **122**, 763-773.
Feinberg, E. H., VanHoven, M. K., Bendesky, A., Wang, G., Fetter, R. D., Shen, K. and Bargmann, C. I. (2008). GFP Reconstitution Across Synaptic Partners (GRASP) defines cell contacts and synapses in living nervous systems. *Neuron* **57**, 353-363.
Fischer, J. A., Giniger, E., Maniatis, T. and Ptashne, M. (1988). GAL4 activates transcription in *Drosophila*. *Nature* **332**, 853-856.
Frankfort, B. J., Nolo, R., Zhang, Z., Bellen, H. and Mardon, G. (2001). senseless repression of rough is required for R8 photoreceptor differentiation in the developing *Drosophila* eye. *Neuron* **32**, 403-414.
Fu, W., Duan, H., Frei, E. and Noll, M. (1998). shaven and sparkling are mutations in separate enhancers of the *Drosophila* Pax2 homolog. *Development* **125**, 2943-2950.
Golic, K. G. (1991). Site-specific recombination between homologous chromosomes in *Drosophila*. *Science* **252**, 958-961.
Gordon, M. D. and Scott, K. (2009). Motor control in a *Drosophila* taste circuit. *Neuron* **61**, 373-384.
Hadjieconomou, D., Rotkopf, S., Alexandre, C., Bell, D. M., Dickson, B. J. and Salecker, I. (2011). Flybow: genetic multicolor cell labeling for neural circuit analysis in *Drosophila melanogaster*. *Nat. Methods* **8**, 260-266.
Haigo, S. L. and Bilder, D. (2011). Global tissue revolutions in a morphogenetic movement controlling elongation. *Science* **331**, 1071-1074.
Hampel, S., Chung, P., McKellar, C. E., Hall, D., Looger, L. L. and Simpson, J. H. (2011). *Drosophila* Brainbow: a recombinase-based fluorescence labeling technique to subdivide neural expression patterns. *Nat. Methods* **8**, 253-259.
Hsiung, F., Ramirez-Weber, F.-A., Iwaki, D. D. and Kornberg, T. B. (2005). Dependence of *Drosophila* wing imaginal disc cytonemes on Decapentaplegic. *Nature* **437**, 560-563.
Ito, K., Awano, W., Suzuki, K., Hiromi, Y. and Yamamoto, D. (1997). The *Drosophila* mushroom body is a quadruple structure of clonal units each of which contains a virtually identical set of neurones and glial cells. *Development* **124**, 761-771.
Johnston, L. A., Prober, D. A., Edgar, B. A., Eisenman, R. N. and Gallant, P. (1999). *Drosophila* myc regulates cellular growth during development. *Cell* **98**, 779-790.
Kim, J., Zhao, T., Petralia, R. S., Yu, Y., Peng, H., Myers, E. and Magee, J. C. (2012). mGRASP enables mapping mammalian synaptic connectivity with light microscopy. *Nat. Methods* **9**, 96-102.
Lai, S.-L. and Lee, T. (2006). Genetic mosaic with dual binary transcriptional systems in *Drosophila*. *Nat. Neurosci.* **9**, 703-709.
Lee, J. D., Amanai, K., Shearn, A. and Treisman, J. E. (2002). The ubiquitin ligase Hyperplastic discs negatively regulates hedgehog and decapentaplegic expression by independent mechanisms. *Development* **129**, 5697-5706.
Livet, J., Weissman, T. A., Kang, H., Draft, R. W., Lu, J., Bennis, R. A., Sanes, J. R. and Lichtman, J. W. (2007). Transgenic strategies for combinatorial expression of fluorescent proteins in the nervous system. *Nature* **450**, 56-62.
Martin-Castellanos, C. and Edgar, B. A. (2002). A characterization of the effects of Dpp signaling on cell growth and proliferation in the *Drosophila* wing. *Development* **129**, 1003-1013.
Marygold, S. J., Roote, J., Reuter, G., Lambertsson, A., Ashburner, M., Millburn, G. H., Harrison, P. M., Yu, Z., Kenmochi, N., Kaufman, T. C. et al. (2007). The ribosomal protein genes and *Minute* loci of *Drosophila melanogaster*. *Genome Biol.* **8**, pR216.
Morata, G. and Ripoll, P. (1975). Minutes: mutants of drosophila autonomously affecting cell division rate. *Dev. Biol.* **42**, 211-221.
Moreno, E. and Basler, K. (2004). dMyc transforms cells into super-competitors. *Cell* **117**, 117-129.
Neely, G. G., Kuba, K., Cammarato, A., Isobe, K., Amann, S., Zhang, L., Murata, M., Elmén, L., Gupta, V., Arora, S. et al. (2010). A global in vivo *Drosophila* RNAi screen identifies NOT3 as a conserved regulator of heart function. *Cell* **141**, 142-153.
Newsome, T. P., Asling, B. and Dickson, B. J. (2000). Analysis of *Drosophila* photoreceptor axon guidance in eye-specific mosaics. *Development* **127**, 851-860.
Ni, J.-Q., Zhou, R., Czech, B., Liu, L.-P., Holderbaum, L., Yang-Zhou, D., Shim, H.-S., Tao, R., Handler, D., Karpowicz, P. et al. (2011). A genome-scale shRNA resource for transgenic RNAi in *Drosophila*. *Nat. Methods* **8**, 405-407.
Nystul, T. and Spradling, A. (2010). Regulation of epithelial stem cell replacement and follicle formation in the *Drosophila* ovary. *Genetics* **184**, 503-515.
Orenic, T. V., Slusarski, D. C., Kroll, K. L. and Holmgren, R. A. (1990). Cloning and characterization of the segment polarity gene cubitus interruptus Dominant of *Drosophila*. *Genes Dev.* **4**, 1053-1067.
Pignoni, F. and Zipursky, S. L. (1997). Induction of *Drosophila* eye development by decapentaplegic. *Development* **124**, 271-278.
Pospisilik, J. A., Schramek, D., Schnidar, H., Cronin, S. J. F., Nehme, N. T., Zhang, X., Knauf, C., Cani, P. D., Aumayr, K., Todoric, J. et al. (2010). *Drosophila* genome-wide obesity screen reveals hedgehog as a determinant of brown versus white adipose cell fate. *Cell* **140**, 148-160.
Potter, C. J., Tasic, B., Russler, E. V., Liang, L. and Luo, L. (2010). The Q system: a repressible binary system for transgene expression, lineage tracing, and mosaic analysis. *Cell* **141**, 536-548.
Qian, X. H. and Cox, M. M. (1995). Asymmetry in active complexes of FLP recombinase. *Genes Dev.* **9**, 2053-2064.
Quinn, L. M., Herr, A., McGarry, T. J. and Richardson, H. (2001). The *Drosophila* Geminin homolog: roles for Geminin in limiting DNA replication, in anaphase and in neurogenesis. *Genes Dev.* **15**, 2741-2754.
Ready, D. F., Hanson, T. E. and Benzer, S. (1976). Development of the *Drosophila* retina, a neurocrystalline lattice. *Dev. Biol.* **53**, 217-240.
Rezával, C., Werbajh, S. and Ceriani, M. F. (2007). Neuronal death in *Drosophila* triggered by GAL4 accumulation. *Eur. J. Neurosci.* **25**, 683-694.
Ringrose, L., Chabanis, S., Angrand, P.-O., Woodroofe, C. and Stewart, A. F. (1999). Quantitative comparison of DNA looping in vitro and in vivo: chromatin increases effective DNA flexibility at short distances. *EMBO J.* **18**, 6630-6641.
Schlake, T. and Bode, J. (1994). Use of mutated FLP recognition target (FRT) sites for the exchange of expression cassettes at defined chromosomal loci. *Biochemistry* **33**, 12746-12751.
Schnutgen, F., De-Zolt, S., Van Sloun, P., Hollatz, M., Floss, T., Hansen, J., Altschmied, J., Seisenberger, C., Ghyselinck, N. B., Ruiz, P. et al. (2005). Genomewide production of multipurpose alleles for the functional analysis of the mouse genome. *Proc. Natl. Acad. Sci. USA* **102**, 7221-7226.
Senecoff, J. F. and Cox, M. M. (1986). Directionality in FLP protein-promoted site-specific recombination is mediated by DNA-DNA pairing. *J. Biol. Chem.* **261**, 7380-7386.
Simon, J., Chiang, A. and Bender, W. (1992). Ten different Polycomb group genes are required for spatial control of the abdA and AbdB homeotic products. *Development* **114**, 493-505.
St Johnston, D. (2002). The art and design of genetic screens: *Drosophila melanogaster*. *Nat. Rev. Genet.* **3**, 176-188.
Struhl, G. and Basler, K. (1993). Organizing activity of wingless protein in *Drosophila*. *Cell* **72**, 527-540.
Szuts, D. and Bienz, M. (2000). LexA chimeras reveal the function of *Drosophila* Fos as a context-dependent transcriptional activator. *Proc. Natl. Acad. Sci. USA* **97**, 5351-5356.
Tapon, N., Ito, N., Dickson, B. J., Treisman, J. E. and Hariharan, I. K. (2001). The *Drosophila* tuberous sclerosis complex gene homologs restrict cell growth and cell proliferation. *Cell* **105**, 345-355.
Treisman, J. (2001). Drosophila homologues of the transcriptional coactivation complex subunits TRAP240 and TRAP230 are required for identical processes in eye-antennal disc development. *Development* **128**, 603-615.
Tseng, A.-S. K., Tapon, N., Kanda, H., Cigizoglu, S., Edelmann, L., Pellock, B., White, K. and Hariharan, I. K. (2007). Capicua regulates cell proliferation downstream of the receptor tyrosine kinase/ras signaling pathway. *Curr. Biol.* **17**, 728-733.
Turan, S., Zehe, C., Kuehle, J., Qiao, J. and Bode, J. (2013). Recombinase-mediated cassette exchange (RMCE) - a rapidly-expanding toolbox for targeted genomic modifications. *Gene* **515**, 1-27.
White, K., Grether, M. E., Abrams, J. M., Young, L., Farrell, K. and Steller, H. (1994). Genetic control of programmed cell death in *Drosophila*. *Science* **264**, 677-683.
Xu, T. and Rubin, G. M. (1993). Analysis of genetic mosaics in developing and adult *Drosophila* tissues. *Development* **117**, 1223-1237.
Yang, C. H., Simon, M. A. and McNeill, H. (1999). mirror controls planar polarity and equator formation through repression of fringe expression and through control of cell affinities. *Development* **126**, 5857-5866.

Supplemental Materials and Methods

Construction of the CoinFLP systems

CoinFLP constructs were constructed using traditional cloning techniques and inserted in attP40 on chromosome II using PhiC31 integration (BestGene).

To construct the plasmid used for *CoinFLP-Gal4*, we first PCR amplified the Gal4 coding sequence from pAct-FRT-CD2-FRT-Gal4 (Pignoni and Zipursky, 1997). Multiple restriction sites were added to the 5' end (Fse1-Not1-Age1-EcoRI-BglII) and Kpn1 to the 3' end with forward and reverse primers, respectively (sequence below). We ligated the resulting Gal4 fragment into pAct-FRT-stop-FRT-SV40polyA attB (Brittle et al., 2010), which had been purified after digesting with Fse1 and Kpn1. The resulting plasmid was named pAct-FRT-stop-Gal4 attB, which contains only one FRT site downstream of the *Actin5c* promoter. We ordered a plasmid containing a synthesized region containing two FRT3 sites that flank a wild-type FRT site (Integrated DNA Technologies (IDT)), called pNot1-FRT3-FRT-FRT3-EcoRI. This plasmid was cut with Not1/EcoRI to release FRT3-FRT-FRT3, which was ligated into pAct-FRT-stop-Gal4 attB. The resulting plasmid was named pAct-FRT-stop-FRT3-FRT-FRT3-Gal4 attB (Fig. S5) and was used to generate transgenic flies. This plasmid has been deposited with Addgene (52889).

To construct the plasmid used for CoinFLP-LexGAD/Gal4, we first ordered a plasmid from (IDT) containing the following elements from 5' to 3': FRT and FRT3 sites, a transcriptional stop sequence, a FRT site, a multiple cloning site containing EcoRI-Age1-Not1, and a FRT3 site. This plasmid was named pXho1-FRT-FRT3-stop-FRT-EcoRI-Age1-Not1-FRT3-BglII. We PCR amplified LexGAD coding and Hsp70 polyA sequence from pBPnlsLexA::GADflUw (Pfeiffer et al., 2010), adding EcoRI to 5' end and Not1 to 3' end with primers (sequence below). This PCR fragment was ligated into pXho1-FRT-FRT3-stop-FRT-EcoRI-Age1-Not1-FRT3-BglII with EcoRI/Not1. The resulting plasmid was named pXho1-FRT-FRT3-stop-FRT-LexGAD-FRT3-BglII. This plasmid was cut with Xho1/BglII and the released fragment was ligated into pAct-

FRT-stop-Gal4 attB cut with PspXI/BglII (the digested backbone lacks the FRT-stop sequence). The resulting plasmid is named pAct-FRT-FRT3-stop-FRT-LexGAD-FRT3-Gal4 attB (Fig. S6) and was used to generate transgenic flies. This plasmid has been deposited with Addgene (52890).

Oligonucleotides used (lower case = sequence added 5' to primer)
Fse1-Not1-Age1-EcoRI-BglII-Gal4-F
cgcgggccggccagcggccgcaccggtgaattcagatctTAAGCAAATAAACAAGCGCAG
Kpn1-Gal4-R
gcgcggtaccTTACTCTTTTTTTGGGTTTGGTG
EcoRI-LexGAD-F
cgggctgcaggaattccaaaATGCCACCCAAGAAGA
Not1-LexGAD-R
gacgcggcggccgcGATCTAAACGAGTTTTTAAGCAAACTC

Selecting RNAi lines toward genes used for the CoinFLP screen

To compile of list of genes in the genome that are refractory to screening by traditional mosaic analysis (mitotic recombination between *FRT* sites in *trans* on homologous chromosomes), we subtracted a list of genes distal to the commonly used *FRT* sites from the entire genome.

Genes distal to *FRT*s were defined by the known start/stop position of each chromosome arm and the insertion position of each *FRT* (Potter and Luo, 2010). For example, *FRT19A* is inserted at position X:19,804,903 on chromosome X. Genes distal to *FRT19A* are therefore in the range X:1..19,804,903. This was repeated for the four other commonly used *FRT* insertions *FRT40A* (2L:21,794,705), *FRT42D* (2R: 2,760,212), *FRT80B* (3L:23,095,809), and *FRT82B* (3R:278,974). We used QueryBuilder (flybase.org) to subtract this list from a list of all the genes in the genome (genome release 5.44 at the time of this analysis), resulting in a list of 863 genes, 302 of which are predicted protein coding, located in centromeric regions, the 4th chromosome, and the Y chromosome.

TRiP RNAi fly lines were selected based on our list of genes, resulting in 234 lines, targeting 175 different genes. Table S2 lists the TRiP RNAi stocks used.

Supplemental References

Brittle, A. L., Repiso, A., Casal, J., Lawrence, P. A. and Strutt, D. (2010). Four-jointed modulates growth and planar polarity by reducing the affinity of dachsous for fat. *Curr Biol* **20**, 803-810.

Pfeiffer, B. D., Ngo, T. T., Hibbard, K. L., Murphy, C., Jenett, A., Truman, J. W. and Rubin, G. M. (2010). Refinement of tools for targeted gene expression in *Drosophila*. *Genetics* **186**, 735-755.

Potter, C. J. and Luo, L. (2010). Splinkerette PCR for mapping transposable elements in *Drosophila*. *PLoS One* **5**, e10168.

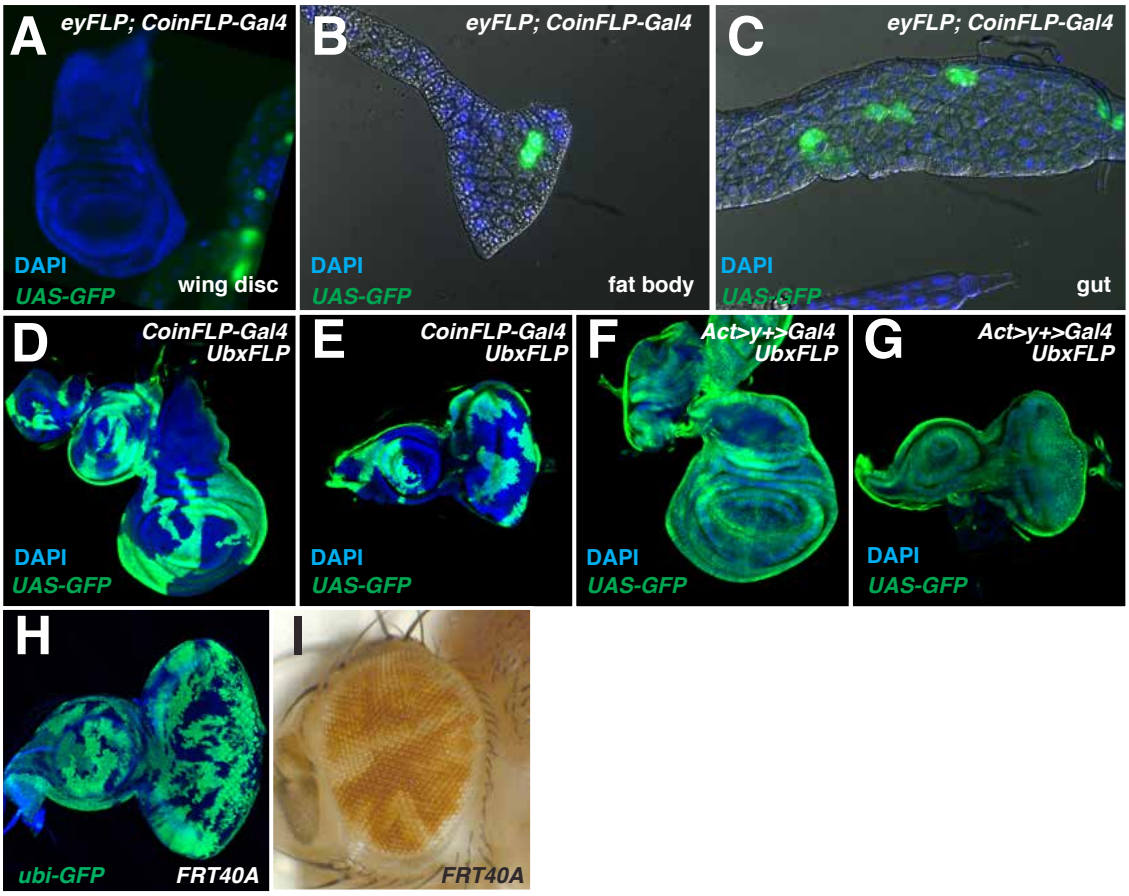

Figure S1: Additional characterization of the CoinFLP-Gal4 system. (A) A wing imaginal disc that does not express *UAS-GFP* when using *CoinFLP-Gal4* with *ey-FLP*. Sporadic expression of *UAS-GFP* in third-instar larvae using *CoinFLP-Gal4* in cells of the (B) fat body and (C) gut. (D-G) *Ubx-FLP*-driven recombination. (D) Haltere, leg, wing discs and (E) eye discs exhibit mosaic expression of *UAS-GFP* using *CoinFLP-Gal4*. (F) Haltere, leg, wing discs and (G) eye discs exhibit uniform expression of *UAS-GFP* using *Act>y+>Gal4*. (H-I) Traditional mitotic recombination between FRT40A sites using *ey-FLP*. (H) Mosaic eye-antennal disc, (I) mosaic adult eye. Genotypes: (A-C) *ey-FLP/+*; *CoinFLP-Gal4 UAS-GFP/+* (D-E) *Ubx-FLP/+*; *CoinFLP-Gal4 UAS-GFP/+* (F-G) *Ubx-FLP/+; Act>y+>Gal4 UAS-GFP/+* (H-I) *ey-FLP/+*; *FRT40A ubi-GFP/FRT40A*

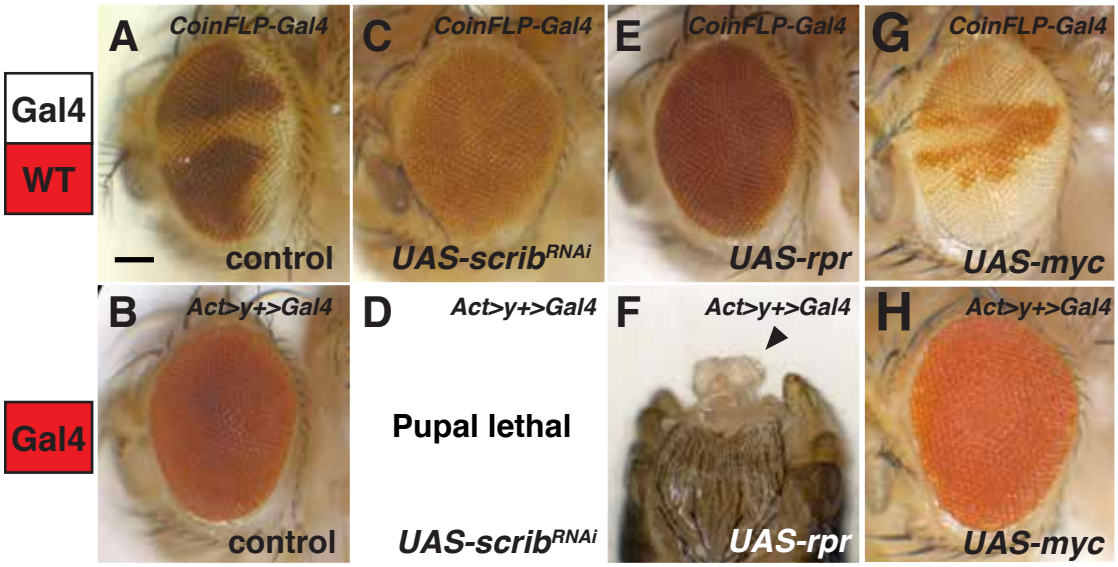

Figure S2: Mosaic eye phenotypes elicited with *CoinFLP-Gal4* and *ey-FLP*. (A-B) Control adult eyes (C-D) *UAS-scrib*^{RNAi}, (E-F) *UAS-rpr*, (G-H) *UAS-Myc*. (A, C, E, G) Mosaic eyes using *CoinFLP-Gal4* and *ey-FLP*. *UAS-white*^{RNAi} marks Gal4 expressing patches as white. (B, D, F, H) Eyes with *Act>y+>Gal4* and *ey-FLP*, uniformly expressing Gal4. Note: This genotype does not contain *UAS-white*^{RNAi} and Gal4 expressing cells are red. (F) Arrow head indicates remaining proboscis after head ablation. Scale bar: (A-H) 100µm. Genotypes: (A, C, E, G) *ey-FLP UAS-dcr2/+; CoinFLP-Gal4 /+; UAS-white*^{RNAi}*/UAS-X* (B, D, F, H)) *ey-FLP UAS-dcr2/+; Act>y+>Gal4 UAS-GFP/+; UAS-X/+*

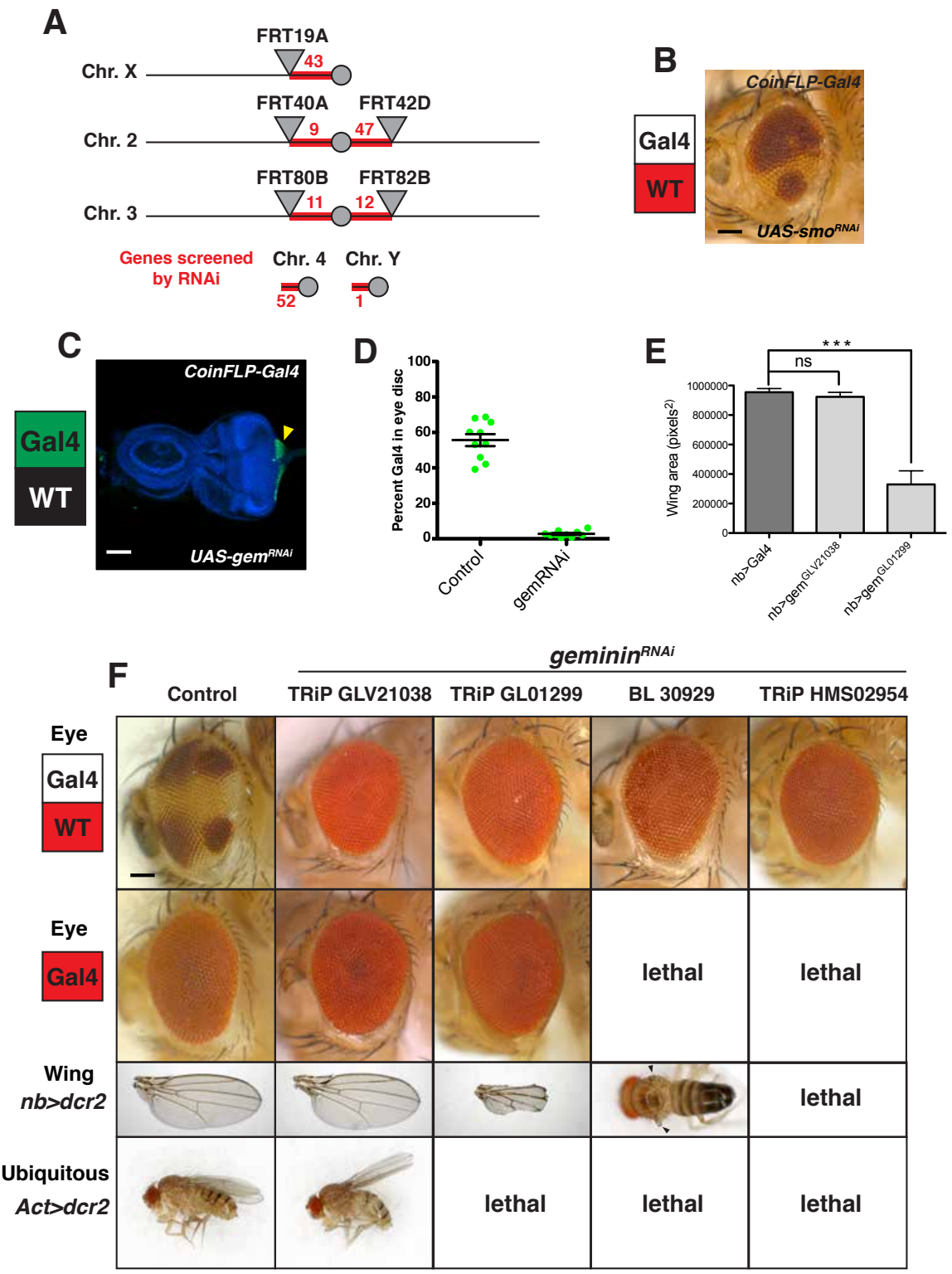

Figure S3: **Additional characterization from *CoinFLP-Gal4* screen.** (A) Locations of genes screened. (B) *UAS-smo*^{RNAi} mosaic adult eye using *CoinFLP-Gal4* and *ey-FLP*. Mutant cells are marked as white with *UAS-white*^{RNAi}. (C) *UAS-gem*^{RNAi} mosaic eye-antennal disc using *CoinFLP-Gal4* and *ey-FLP*. Mutant cells are marked with *UAS-GFP* (green). (D) Quantification of *UAS-gem*^{RNAi} mutant clone area in the eye-antennal

disc. Mean=3%, N=10 discs, s.d.= 1.6%, p<.001. (E) Quantification adult wing size from expression of *UAS-gem^{RNAi}* in the wing imaginal disc. N=30 wings, *** = p<.001 (F) Adult phenotypes from expression of different *UAS-gem^{RNAi}* transgenes. The lines are shown from left to right in order of increasing severity of phenotypes: TRiP GLV21038 < TRiP GL01299 < BL 30929 < TRiP HMS02954. Scale bar: (B-C, F) 100µm. Genotypes: (B) *ey-FLP UAS-dcr2/+; CoinFLP-Gal4 /+; UAS-white^{RNAi}/UAS-smo^{RNAi}* (C) *ey-FLP UAS-dcr2/+; CoinFLP-Gal4 UAS-GFP/+; +/UAS-gem^{RNAi}* (F) 1st row: *ey-FLP UAS-dcr2/+; CoinFLP-Gal4 /+; UAS-white^{RNAi}/UAS-X* 2nd row: *ey-FLP UAS-dcr2/+; Act>y+>Gal4 UAS-GFP/+; UAS-X/+* 3rd row: *UAS-dcr2/+; nb-Gal4/+; UAS-X/+* 4th row: *UAS-dcr2/+; act-Gal4/+; UAS-X/+*

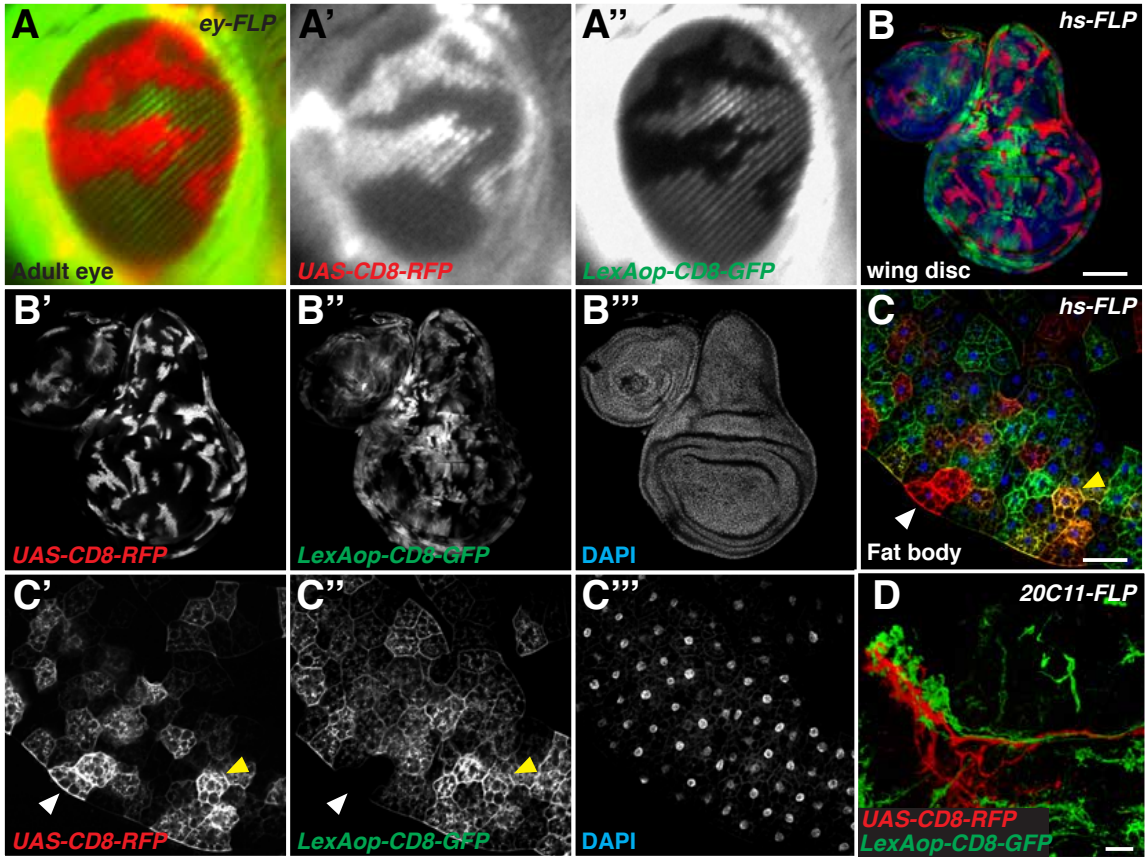

Figure S4: **Additional characterization of CoinFLP-LexGAD/Gal4 system.** (A-D) Tissues with *CoinFLP-LexGAD/Gal4* and different FLP transgenes. LexGAD expressing cells are marked with *LexAop-CD8-GFP* (green) and Gal4 cells with *UAS-CD8-RFP* (red). (A-A'') Adult eyes composed of only Gal4 or LexGAD clones using *ey-FLP*. Anterior is to the left. (B-B''') Confocal section showing Gal4- and LexGAD-expressing clones generated in the wing disc and (C-C''') fat body. White arrowhead indicates a cell expressing predominantly Gal4 while the yellow arrowhead indicates a cell that expresses both Gal4 and LexGAD. (D)Two neighboring neurons, each expressing either Gal4 or LexGAD induced by *20C11-FLP*. Scalebar: (B-C''') 100µm, (D) 10µm. Genotypes: (A) *ey-FLP/UAS-CD8-RFP, lexAop-CD8-GFP; CoinFLP-LexGAD|Gal4/+* (B) *sens-FLP/UAS-CD8:RFP, LexAop-CD8:GFP; CoinFLP-LexGAD|Gal4/+* (C-D''') *hs-FLP/UAS-CD8:RFP, LexAop-CD8:GFP; CoinFLP-LexGAD|Gal4/+* (E) *20C11-FLP (Chr.?)/UAS-CD8:RFP, LexAop-CD8:GFP; CoinFLP-LexGAD|Gal4/+*

```
        Actin P.                    PspXI
CTAGTGGATCAGCTTGCATGCCTGCAGGTCCCCTCGAGGGGACTCTAGCTAGAGGATCC

                    FRT
CGGAAGTTCCTATTCTCTAGAAAGTATAGGAACTTCGAATTGACTAAAGCCAAATAGAA

AATTATTCAGTTCCTGGCTTAAGTTTTTAAAAGTGATATTATTTATTTGGTTGTAACCA

                         Hsp70 3'UTR ("Stop")
ACCAAAAGAATGTAAATAACTAATACATAATTATGTTAGTTTTAAGTTAGCAACAAATT

GATTTTAGCTATATTAGCTACTTGGTTAATAAATAGAATATATTTATTTAAAGATAATT

GCGTTTTTATTGTCAGGGAGTGAGTTTGCTTAAAAACTCGTTTAGATCCACTAGTTCTA

        FseI      Not1
GTTGCGGCCGGCCAGCGGCCGCTGGGTTCAGGCATAGAGGAGTTGACGACTACTTCCAA

GGCAGTACGTGACGTAACGGCCCTTAAAGTGATCAGTCCTTATTGCTTTGTCTGCCGGA

               FRT3
AGTTCCTATTCTTCAAATAGTATAGGAACTTCGTGTGAGGGAGCGTATTTGGGAAGTTC

              FRT
CTATTCTCTAGAAAGTATAGGAACTTCCCCGCTTACCACCATACATCCAAATCACTACG

                            FRT3
GCTCGCTTGAAGTTCCTATTCTTCAAATAGTATAGGAACTTCGATGGTGTAGTGTTGCG

   EcoRI  BglII
GTGGAATTCAGATCTTAAGCAAATAAACAAGCGCAGCTGAACAAGCTAAACAATCTGCA

                               Gal4(2646bp) Kpn1     SV40 3'UTR
GCCCAAGCTTGAAGCAAGCCTCCTGAAAGATG...TAAGGTACCTAGATCT...TCT
```

Figure S5: DNA sequence of the CoinFLP-Gal4 transgene. Sequence displayed corresponds to the 3' end of the Actin promoter through the SV40 3'UTR in the pAct-FRT-stop-FRT3-FRT-FRT3-Gal4 attB plasmid. Bold underlined text indicates restriction enzyme sites that are unique in the plasmid.

```
        Actin P.                    Xho1            FRT
CTAGTGGATCAGCTTGCATGCCTGCAGGTCCCCTCGAGGAAGTTCCTATTCTCTAGAAA

                                                  FRT3
GTATAGGAACTTCCCCGCGTACCACCAGACAGCGAAGTTCCTATTCTTCAAATAGTATA

GGAACTTCGAATTGACTAAAGCCAAATAGAAAATTATTCAGTTCCTGGCTTAAGTTTTT

AAAAGTGATATTATTTATTTGGTTGTAACCAACCAAAAGAATGTAAATAACTAATACAT

                        Hsp70 3'UTR ("Stop")
AATTATGTTAGTTTTAAGTTAGCAACAAATTGATTTTAGCTATATTAGCTACTTGGTTA

ATAAATAGAATATATTTATTTAAAGATAATTGCGTTTTTATTGTCAGGGAGTGAGTTTG

CTTAAAAACTCGTTTAGATCCACTAGTTCTAGTTGCGGCCGGCCGCAACTAGAGGATCC

                    FRT                     EcoRI   LexGAD(2853bp)
CGGAAGTTCCTATTCTCTAGAAAGTATAGGAACTTCGAATTCCAAAATG...TAGGTTT

Pmel        Hsp70 3'UTR(246bp) Not1          FRT3
AAACAAGCTTATCGATACCGTC...ATCGCGGCCGCGAAGTTCCTATTCTTCAAATAGT

            BglII
ATAGGAACTTCAGATCTTAAGCAAATAAACAAGCGCAGCTGAACAAGCTAAACAATCTG

                                Gal4(2646bp) Kpn1   SV40 3'UTR
CAGCCCAAGCTTGAAGCAAGCCTCCTGAAAGATG...TAAGGTACCTAGATCT...TCT

BamHI
GGATCC
```

Figure S6: DNA sequence of the CoinFLP-LexGAD/Gal4 transgene. Sequence displayed corresponds to the 3' end of the Actin promoter through the SV40 3'UTR in the pAct-FRT-FRT3-stop-FRT-LexGAD-FRT3-Gal4 attB plasmid. Bold underlined text indicates restriction enzyme sites that are unique in the plasmid.

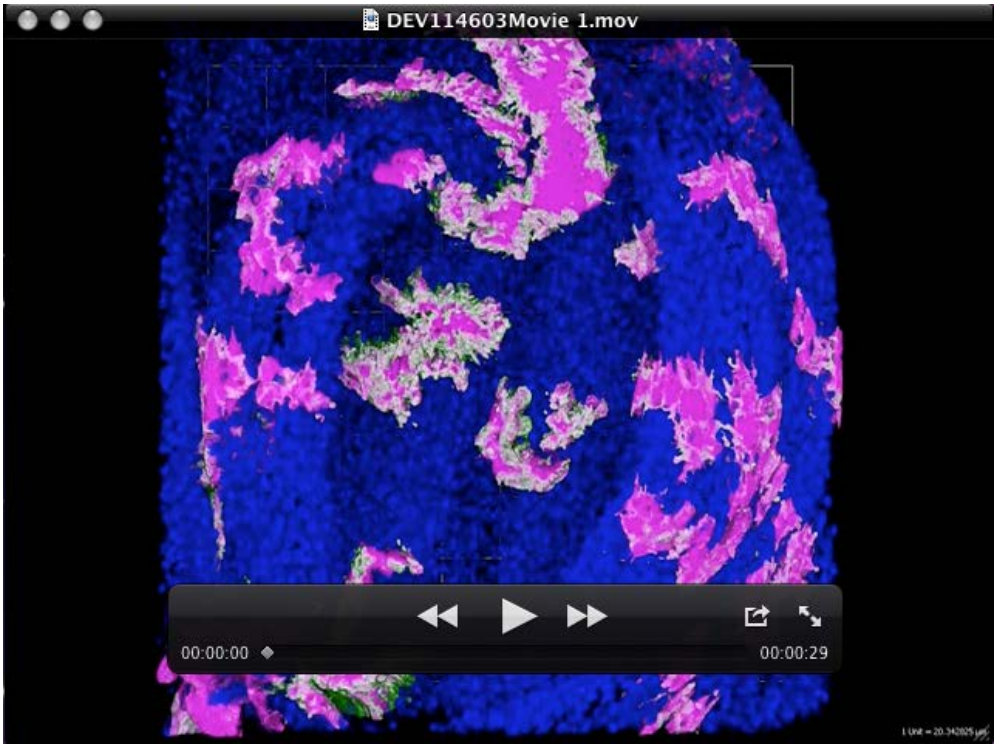

Movie 1: 3D reconstruction and flyc through of cell contacts in the wing disc. Wing imaginal disc with clone boundaries marked by GRASP. Clones expressing spGFP1t 10 are labeled magenta, GRASP fluorescence is green, and nuclei are labeled with DAPI (blue). spGFP11 clones are not labeled and nearly surround spGFP1-10 clones. A confocal stack of the pouch of a 3rd instar wing imaginal disc was processed with Volocity software to produce a 3D reconstruction and fly-through to better visualize the extent of cell contact visualized by GRASP. Genotype: *hs-FLP/+; CoinFLP-LexGAD|Gal4, LexAop-CD2-RFP/+; UAS-CD4-spGFP1-10, LexAop-CD4-spGFP11/+*

Table S1.xls: **Comparison of different *eyFLP* transgenes in the context of the CoinFLP system.** Expression of Gal4 is induced by *eyFLP* transgenes when paired with either *Act>y+>Gal4* or *CoinFLP-Gal4* transgenes. A *UAS-GFP* was included to visualize Gal4 expression. Several tissues in the 3rd instar larvae were inspected for GFP expression with the different *ey-FLP* transgenes. *ey-FLP* in stock #BL5580 has the most restricted expression in the eye imaginal disc.

Click here to Download Table S1

Table S2.xls: *CoinFLP-Gal4* screen phenotypes elicited by UAS-RNAi. List of adult phenotypes induced by RNAi of corresponding genes. Adult mosaic eye phenotypes were identified in a primary screen using *CoinFLP-Gal4*. Adult wing phenotypes were scored in parallel using *nubbin-Gal4*, which expresses Gal4 in the larval wing imaginal disc. For cases in which RNAi expression in the mosaic eye lead to the elimination of mutant tissue, these RNAi lines were scored in a secondary assay that uses uniform Gal4 expression in the eye.

Click here to Download Table S2

Table S3.xls: Useful *CoinFLP-Gal4* and *CoinFLP-LexGAD/Gal4* stocks. List of Drosophila stocks for conducting experiments using the *CoinFLP-Gal4* and *CoinFLP-LexGAD/Gal4* transgenes.

Click here to Download Table S3